Understanding the effects of nanoporous titanium on osteoblastic cells in hyperglycemic conditions

Thesis submitted to the University of Ottawa in partial fulfilment of the requirements for the
Master of Applied Science

by
Nidhi Narendra Agrawal

Department of Biomedical Engineering
Faculty of Engineering
University of Ottawa

uOttawa

DECLARATION

I hereby declare that the thesis entitled “Understanding the effects of nanoporous titanium on osteoblastic cells in hyperglycemic conditions,” submitted by me for the award of the degree of Master of Applied Science from the University of Ottawa, is a record of bonafide work carried out by me under the supervision of Dr. Fabio Variola, Professor, Faculty of Engineering, University of Ottawa.

I further declare that the work reported in this thesis has not been submitted and will not be submitted, either in part or in full, for the award of any other degree or diploma in this institute or any other institute or university.

The complete study was designed and executed in its entirety by myself, and I am the sole author of relevant written work.

ABSTRACT

Towards the creation of the next generation of biomedical implants that effectively integrate in tissues, understanding cell behaviour at the material-host interface to control and optimize the biological outcome is a crucial endeavour. It is now well-known that the nanoscale surface properties of biomaterials play a significant role in directing the activity of adherent cells at the implant-host tissue interface. A variety of cellular functions, ranging from adhesion and proliferation to differentiation along specific lineages, are guided by the nanoscale topographical and physicochemical features of the substrate. This evidence reaffirms the role of surface features on eliciting an enhanced response of cells towards improved biological outcomes (e.g., bone integration) of implanted biomaterials. In this context, Titanium (Ti) and its alloys are popular biomaterials widely used in orthopedic, dental, and cardiovascular applications. In particular, in the field of osseointegrated devices, chemical treatments of titanium, specifically oxidative nanopatterning (i.e., a simple yet effective treatment with a H_2SO_4/H_2O_2 solution), have shown to be a promising strategy for guiding and controlling the fate of relevant cells (e.g., osteoblasts, stem cells), thereby achieving the ability to direct the biological response towards the desired outcome. In this context, the sponge-like nanoporous surface resulting from oxidative nanopatterning of titanium allows direct surface cueing to bone cells. It also has the capacity to selectively regulate cell behaviour, modulate the expression of crucial determinants of cell activity, and offers the potential to harness the power of stem cells. However, the mechanisms that control how cells sense and respond to these nanometric cues are still elusive. A novel strategy to elucidate them takes inspiration from *in-vivo* protocols, where "knock-out" animal models are used to determine the role of a specific gene. Based on this, I propose an original approach aimed at investigating cell response under conditions known to affect specific cellular processes, thereby determining whether these activities can be rescued by direct cueing by the substrate, ultimately elucidating their implication in responding to a given nanostructured substrate. In particular, hyperglycemic culturing conditions often used to mimic diabetes *in-vitro* are known to exert detrimental effects on the proliferation and differentiation of osteoblasts, and thereby could be an excellent opportunity to test whether the nanometric surface features resulting from oxidative nanopatterning of titanium also possess the ability to compensate to the cell-level changes caused by higher levels of glucose. This would ultimately demonstrate a direct effect of the

substrate on these events and help us understand the mechanisms involved in cell-biomaterial interactions.

To address this challenge, I propose to investigate the response of human MG-63 osteoblastic cells to nanoporous titanium under hyperglycemic conditions. The goal is, therefore, to understand whether direct nanotopographical cueing at the nanoscale can rescue MG-63 cells from the effects of hyperglycemia, thereby casting new light on the mechanisms underlying the interactions between this widely used cell line and nanoporous titanium. In parallel, results from my work aim at providing new fundamental evidence to interpret results from that body of literature that uses high glucose content as a way to mimic the osseointegration of biomaterials in diabetic conditions.

To my beloved Eva and Eve…

ACKNOWLEDGMENT

I am colossally appreciative to my parents, Mr. Narendra Agrawal and Mrs. Ranjana Agrawal, for their love, affection, and comprehension. Thank you for letting me fly and for trusting in me while I took this big leap in life. This is dedicated to you for always letting me be and for constantly pushing me to achieve whatever I want without any questions in life. I want to thank my brother, Raj Agrawal, for his encouragement and support. It becomes easy with you three in my corner.

My supervisor, Prof. Fabio Variola, to whom I am incredibly grateful for his direction and inspiration. You have helped me immensely throughout the entire journey and allowed me to take decisions on my own. Thank you for providing an international student with this opportunity; it helped me gain a deeper understanding of the biomedical engineering field. Variola research group allowed me the research freedom and the funds for which I am extremely thankful.

I want to thank Alexander Steeves for his guidance and for entertaining all my questions and doubts, and for teaching me all his great techniques during my time in the lab. I would also like to thank Dr. Alp Ozgun for guiding, helping me and being so present while teaching me. Thank you also to David Lomboni, Ryan Berthelot and Roja Gauda for their presence and support during my graduate studies.

I want to acknowledge the help and support of Dr. Chloe Van Oostende-Triple and the staff at the uOttawa CBIA Microscopy Core for training me in fluorescence microscopy and image analysis. I also am thankful to Dr. William Staines for allowing me in his laboratory to conduct my experiments.

And finally, I would like to thank my friends who became my big fat Canadian family. Being away from family in a new country was not an easy journey, but they were always there for me, in good times and bad. To them, I am immensely grateful for all the support, food (looking at you, Priti) and adventures that made me always feel at home.

TABLE OF CONTENTS

LIST OF FIGURES

LIST OF ABBREVIATIONS AND ACRONYMS

ALP	Alkaline Phosphatase
ANOVA	Analysis of Variance
BSP	Bone sialoprotein
CTRL	Control(condition)
DAPI	4,6-Diamidino-2-Phenylindole
DI	Deionised water
DM	Diabetes Mellitus
DMEM	Dulbecco's Modified Eagle Medium
ECM	Extracellular matrix
EtOH	Ethyl alcohol
FBS	Fetal Bovine Serum
HCl	Hydrochloric acid
HF	Hydrofluoric acid
H_2O_2	Hydrogen Peroxide

H_2SO_4	Sulfuric Acid
MSCs	Mesenchymal Stem Cells
NPTi	Nanoporous Titanium
OCN	Osteocalcin
OPN	Osteopontin
PBS	Phosphate Buffered Saline
PFA	Paraformaldehyde
RT	Room temperature
RUNX2	Runt-related transcription factor 2
SEM	Scanning Electron Microscopy
TiO_2	Titanium dioxide
WB	Western Blotting

Chapter 1

MOTIVATION, OBJECTIVES AND HYPOTHESES

1.1 Context

Endowing surfaces of biomaterials with nanoscale features have been shown to improve their bioactivity[1]–[5]. In this regard, researchers in the field of osseointegrated implants have been utilizing nanoscale surface modifications to reduce healing time, promote osteointegration and increase the life expectancy of implants[6]–[9]. Titanium has been the gold standard for biomedical implants for a long time due to its mechanical properties, high strength-to-weight ratio, exceptional biocompatibility, and high corrosion resistance[10], [11]. However, to create even more effective titanium implants, a large array of surface modification techniques have been developed to enhance cell adhesion, migration, proliferation, differentiation and, ultimately, osseointegration[12]–[15]. In this context, nanoscale modifications based on the use of chemical etchants have shown great potential in increasing biocompatibility [14]–[17]. Acid etching, alkali-heat treatment, and anodization are a few techniques that have been widely employed to achieve this goal[19]–[22]. However, the mechanisms employed to bring about these modifications remain unclear[23]. In this context, Nanci *et al.* [9] demonstrated a protocol to create nanoporous surfaces on titanium using a simple yet effective chemical treatment, namely oxidative nanopatterning. The controlled chemical oxidation leads to the modification of the outer oxide layer, which enhances the biological activity of the surface by selectively controlling protein adsorption[24] and uniquely promoting the activity of osteoblastic cells while inhibiting that of fibroblastic cells[4], [25], [26]. This nanoporous surface has gained increasing interest due to the ease of reproducibility and the beneficial effects of the treatment on both initial and subsequent osteogenic (bone-forming) events both *in-vitro* [4], [9], [14], [15], [26] and *in-vivo*[27]–[29].

In a more general context, uncontrolled blood glucose remains a contraction in implant therapy[30]–[32], drawing attention to the need for awareness and the generation of implants which can still perform under the changes in hyperglycemic patients[30], [33]–[36]. In this regard, the potential of surface modifications at the nanoscale to resolve this problem must be evaluated.

1.2 Motivation

The present study aims to contribute by analyzing the effects of oxidative nanopatterning of titanium[37] by employing a widely used human osteoblastic cell line, MG-63, in normal and hyperglycemic conditions. In this way, this study will assess whether the nanoporous surface possesses the ability to rescue osteoblastic cells from the detrimental effects of hyperglycemia, thereby contributing to elucidating cell-substrate interactions while supporting the research space that needs increasing clarity on whether surface modifications of implants are still effective in non-ideal conditions, such as hyperglycemia.

1.3 Objectives

Based on these premises, the main objective of my thesis is to determine the role of nanoporous titanium in rescuing osteoblastic cells from the detrimental effects of hyperglycemia. This will help determine whether nanostructured surfaces act on the functions that are impaired by hyperglycemia. To this end, I propose to:

1. Create nanoporous titanium surfaces via oxidative nanopatterning.
2. Employ a widely used human osteoblastic cell line (MG63) in normal and high glucose conditions.
3. Quantify the changes in morphology, proliferation, and differentiation of MG-63 cells on untreated and nanoporous titanium.
4. Compare the cellular differences observed in normal and hyperglycemic conditions.

1.4 Hypothesis

The hypothesis of the work is as follows:

1. The oxidative nanopatterning will produce a nanoporous surface comparable to that reported in previous literature.
2. Nanoporous titanium will lead to a better proliferation of osteoblastic cells in hyperglycemic conditions.
3. Nanoporous titanium will improve osteoblastic cell's differentiation capacity in hyperglycemic conditions.

Chapter 2

LITERATURE REVIEW

2.1 Biological Surface Science

The human body is an intricate biochemical-mechanical system consisting of numerous components that work in harmony across a variety of levels thanks to a highly precise hierarchical organization, ranging from the nanoscale size of proteins to micro- and macroscopic dimensions of tissues and organs[38], [39]. Among the processes that occur at the nanoscale, cell-cell and cell-matrix interactions are fundamental for a wide variety of biological events[40], [41]. These not only control the response to the extracellular matrix but also that to synthetic biomaterials via phenomena like cell attachment, proliferation, differentiation, and gene expression[42]–[44]. This evidence led to the current health-research based on biological surface science, which focuses on rationally endowing surfaces with nanoscale features for the development of biomaterials with improved bioactivity[45]–[47]. Over the years, this field has seen huge advancements in the development of surface modification techniques to beneficially guide the biological process on metallic, polymeric and ceramic biomaterials towards a pre-determined pathway[46]–[49]. Because of their wide use in implantology, metals, and in particular titanium, the gold standard for osseointegrated implants, have received particular attention in this regard, with specific nanoscale surface modifications aimed at providing an enhanced integration in bone[8], [15], [50], [51].

2.2 Orthopedic Implant materials

Orthopedic implants have been successfully used for decades to replace or repair damaged bones and joints[52]–[54]. The advancement in metals for orthopedic implants has seen tremendous growth in the past decades[55]–[57]. However, due to intrinsic limitations such as the lack of native bioactivity, corrosion and wear, a sub-optimal biological outcome may develop and ultimately negatively affect the implant's performance in the long term [54], [58]. In turn, this has led to the continuous rise in demand for new and improved implant materials that are tough, corrosion- and wear-resistant, bioactive, and able to endure long periods without failing[11], [59], [60].

2.2.1 Titanium

Titanium and its alloys (e.g. Ti-6Al-4V) have emerged as the number one choice for orthopedic and dental implants and have been used extensively for decades due to their excellent combination of strength, fatigue strength, low modulus and biocompatibility[10], [50], [61]. Titanium has been shown to offer low cytotoxicity and is non-carcinogenic[62]. Furthermore, the spontaneous formation of a stable and protective titanium oxide (TiO_2) surface layer due to air-induced passivation makes it corrosion-resistant[63], [64]. In addition, the TiO_2 layer also provides the surface with a moderate charge at physiological pH, which is believed to enhance bioactivity[65], [66]. The presence of this charge has shown that protein denaturation will not occur upon the interactions with the hydrophilic outer shell of proteins[65], [66]. This negative charge is also expected to attract Ca^{2+} ions when exposed to body fluids, which could be advantageous for osseointegration[67], [68].

Even though titanium has been widely used in medicine, several surface modification techniques have been employed to develop a new generation of implantable metals with enhanced bioactivity, i.e. cell adhesion, migration, proliferation, and differentiation that will ultimately lead to improved osseointegration[6], [23], [57], [66].

2.3 Surface modifications of titanium

The extensive array of surface-modification approaches that have been employed to provide titanium-based implants with new biological functions has been mostly fixated at the nanoscale level[23], [28], [69] as it is quite evident from the literature that nanotopography possesses the ability to influence cellular activity[42]–[44]. It has been shown to not only trigger a distinct set of signalling pathways, thereby affecting the activity of osteogenic cells, but also to enhance osteogenic differentiation[8], [70]. In addition, studies have shown that these changes imparted in cellular activity due to the nanoscale surface modifications have been shown to modulate bone response[71]. This modulation in bone response validates the *in-vivo* performance of nanotopographic implants and promises their clinical efficiency[71].

Depending on the treatment employed, surface-modification approaches are mainly categorized into physical and chemical modifications[23], [28], [69].

2.3.1 Physical Modifications

Biomaterials have been altered through various physical processes to give them new beneficial properties, and these modifications have been demonstrated to favour various biological processes[72], [73]. For instance, a nanoscale modification achieved by a superficial deposition of bioactive layers like TiO_2 and hydroxyapatite using techniques like plasma, electrostatic spray or physical vapor deposition (PVD) led to an enhancement in osteoblastic cell activity and *in-vivo* osseointegration[73], [74]. Formation of nanonodular structure on Ti alloys during PVD of microroughened titanium led to an increase in their *in-vivo* osseointegration in rat femur in comparison to their microtextured metallic counterparts[75].

Laser modification is another technique that has been used to modify the topography of the titanium surface[76]. Nanoscale textures generated using laser modifications on titanium implants led to an increase in their osseointegration[77]. Furthermore, cell proliferation and differentiation effects changed according to the nanogrid structure patterns generated by laser ablation on titanium surfaces[23].

2.3.2 Chemical Modifications

Surface properties of titanium designed by chemical methods have been widely reported to positively affect key biological processes such as protein adsorption, cell proliferation and differentiation[8], [78], [79]. In this context, the use of rationally selected acids and oxidants has proven to be an effective way to modify titanium surfaces at the nanoscale level[4], [8], [70]. In addition, the simplicity and the uniform and efficient access to all surfaces offered by chemical treatments make them an attractive approach for large-scale manufacturing[47].

Chemical modification techniques such as electrochemical oxidation allow nanostructuring of the TiO_2 layer, which can be controlled by modifying treatment parameters such as electrolyte concentration and type, voltage and time [20], [47], [80]. The precise design of surface features via chemical treatments is a prerequisite to attain optical cueing to cellular functions. For example, Steeves *et al.* showed that nanotubular surfaces obtained by anodization affected the quality of bone minerals deposited using differentiated stem cells[12]. Popat *et al.* also reported an increase in proliferation and differentiation in marrow stromal cells isolated from rats[81].

Acid etching is another straightforward surface modification technique that leads to nanoscale topography production on titanium[69], [70]. The surface is immersed in an acid solution using strong acids like sulfuric acid (H_2SO_4), Hydrofluoric acid (HF), and Hydrochloric acid

(HCl)[69], [82], [83]. The nanostructures created by this method have been shown to influence cellular activity like cell migration, adhesion, proliferation and differentiation [19].
Likewise, oxidative nanopatterning is a chemical etching technique that generates nanotopography on titanium surfaces using combinations of strong acids and oxidants and has shown promising results in various aspects[4].

2.4 Oxidative Nanopatterning

Oxidative nanopatterning is a particularly effective method for nanostructuring titanium-based metals which involves the use of etching with combinations of strong acids and oxidants[26], [28], [37], [84]. The mixture of a strong acid like sulphuric acid (H_2SO_4) and a strong oxidant like hydrogen peroxide (H_2O_2), called the Piranha solution, has been shown to yield nanopits of approximately 20 nm diameter on titanium and its alloy (Ti6A4V) [25], [37].
The treatment works by removal of the TiO_2 layer followed by its recreation under controlled conditions, ultimately generating a nanostructured surface layer[37]. In addition, the change in the strength of the piranha solution and the time of exposure allows the control of essential parameters like the wettability, surface morphology and thickness of the TiO_2 layer. Furthermore, this flexibility also extends to the change in the density of -OH (hydroxy) groups on the surface, a factor believed to influence cellular activity by possessing the capacity to control protein adsorption selectively.
Several studies in this regard have shown that the nanoporous surfaces resulting from oxidative nanopatterning treatment exert biological activity and could modulate the expression of critical determinants of cell activity[4], [15], [85]. In addition, they uniquely promoted the activity of osteoblastic cells while inhibiting those of fibroblastic cells[4].
An increased cell adherence, proliferation and expression of major matrix bone proteins such as osteopontin (OPN) and Bone sialoprotein (BSP) was also reported in calvaria-derived cell cultures [15], [26]. In the case of stem cells, accelerated growth and upregulated expression of differentiation markers like alkaline phosphatase (ALP) was observed, indicating the treatment's effect on cell differentiation[15]. The nanopores generated on Ti6A4V alloy due to oxidative nanopatterning also showed an affected cell proliferation of osteoblast-like cells derived from rats (UMR-106) and selective inhibition of fibroblast-like cells derived from embryotic mouse (NIH3T3)[25]. In addition, nanoporous titanium has also proven effective in combating implant-association infections as they have been shown to confer antimicrobial properties to both titanium and medical-grade stainless steels[86], [87].

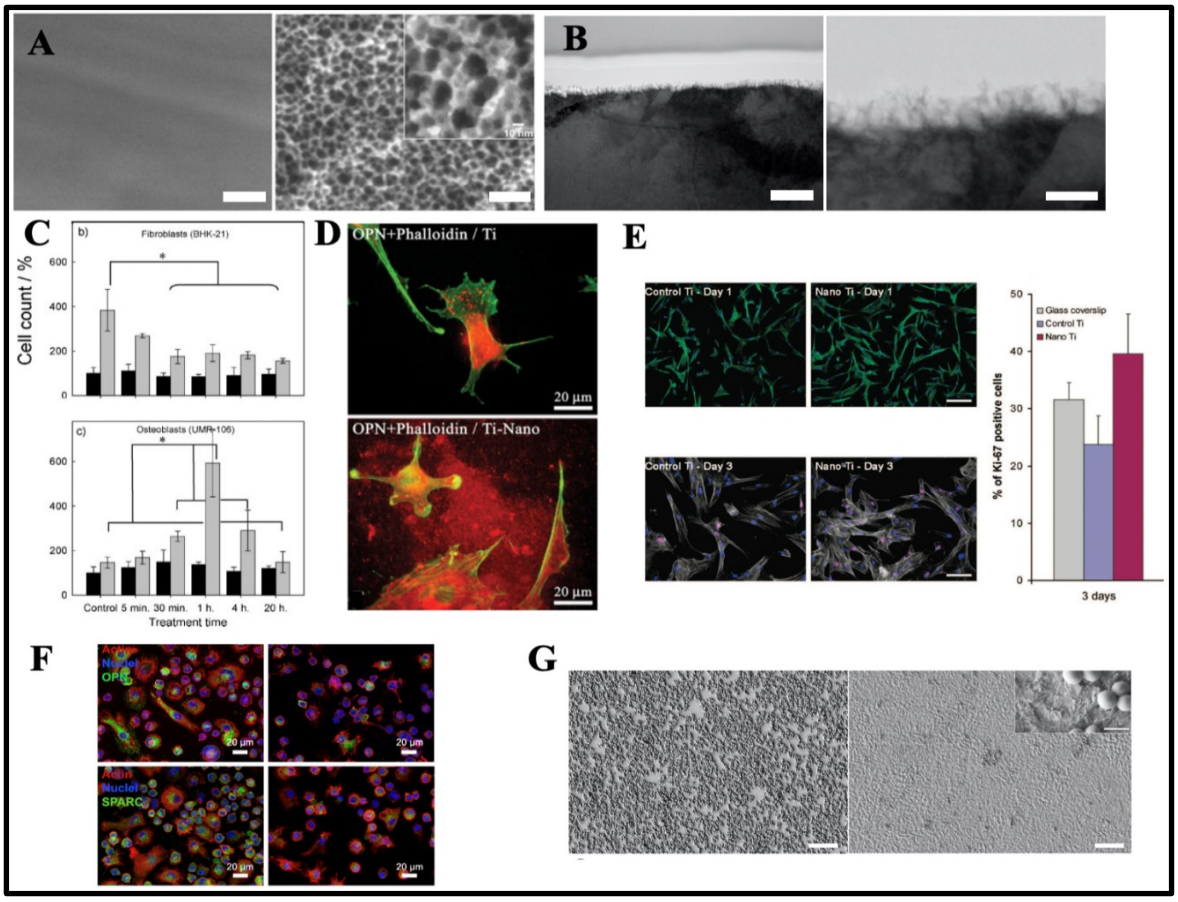

Figure 2.1: Oxidative nanopatterning of titanium and its bioactivity

(A) SEM micrographs of mechanically polished (left) and nanoporous (right) titanium (Ti) surfaces, *Scale bar = 100 nm*[37] *Copyright:© 2006 Elsevier B.V.*. (B) TEM images of FIB ultrathin cross-sectional profile of the nanoporous surface layer, *Scale bar = 100 nm (left), 50 nm (right)*[88] *Copyright © 2014 Variola et al.*. (C) Cell count after 6 h (black bar) and 3 days (gray bar) on control and different treated Ti6Al4V substrates for BHK-21 fibroblasts (top) and UMR-106 osteoblasts[4] *Copyright ©2008 WILEY-VCH Verlag GmbH & Co. KGaA,Weinheim.* (D) Immunolocalization of the matricellular proteins osteopontin (OPN) in primary calvaria-derived osteogenic cells grown on control (top) and nanotextured Ti surfaces bottom)[15] *Copyright ©2009 American Chemical Society*. (E) Human umbilical cord (HUC)-derived cells grown on control Ti surfaces (left) and nanotextured Ti surfaces (right). Areas of higher cell density were frequently observed for nanostructured Ti. Dual nuclear labeling with an anti-Ki-67 antibody and DAPI at day 3 allowed the detection of significantly more cycling cells on nanotextured Ti compared to controls[15] *Copyright ©2009 American Chemical Society*. (F) U937 macrophage protein expression on control (left column) and nanoporous (right column) titanium[89] *Copyright © 2018 Ariganello et al.*. (G) SEM images of Staphylococcus aureus on polished (left) and nanoporous (B, inset) titanium surfaces, *Scale bar = 10 mm*[88] *Copyright © 2014 Variola et al.*.

Furthermore, a decrease in inflammatory response was also reported by Ariganello *et al.,* who studied human immortalized U937-derived macrophage cells exposed to nanocavitated titanium surfaces[89].

In addition, oxidative nanopatterning does not affect the mechanical performance of titanium or the structural integrity of the nanostructured oxide layer, unlike other chemical treatments (such as anodization) used to nanostructure titanium, thereby making it a decent strategy for implanted devices under loading conditions[28].

This extensive research shows that nanoporous titanium obtained by the oxidative nanopatterning method not only offers the ease of reproducibility but also beneficial effects on both, initial and subsequent osteogenic (bone-forming) events. Given these points, this study uses the oxidative nanopatterning treatment proposed by J.-H. Yi *et al.*[37] to further expand on the usage of nanoporous titanium in compromised metabolic conditions like hyperglycemia.

2.5 In vitro cellular assays

An essential aspect of osteo-related research is an effective cell model. It demands a molecular and morphological assessment of the cell line to be employed. Furthermore, choosing a cell model depends on the material's intended application and/or the biological activity to be studied. Many cell lines, such as human Saos-2 and MG63, as well as murine MC3TC3-E1 have been employed in this regard; however, despite their usefulness, they need to be carefully selected in order to facilitate data extrapolation relevant to the intended outcome[90], [91]. For instance, the interspecies difference in MC3T3-E1 cells and the limited mirroring of phenotypic changes in Saos-2 restrain their use in particular studies[92]. MG-63, osteoblasts-like cells, on the other hand, do not possess these restraints and have long been used to assess the *in-vitro* cell behaviour of osteoblasts[92].

2.5.1 MG-63 cells

The MG-63 cell line has been employed in several osteo-based biological studies for experimental modelling. They are derived from a 14-year-old male's osteosarcoma. These cells exhibit an immature osteoblast phenotype and undergo a temporal development when cultured for longer[92]. These cells divide rapidly, thereby displaying the ease of culturing with limitless growth. Furthermore, the congruity of integrin-subunits allows for simple cell-substrate studies[92]. They have also been shown to regulate various functions in osteogenesis and have been used in various studies to understand the expression of osteoblastic markers[90]. Overall,

making them an optimal choice for osteoblast-like experimental modelling of biomaterials that interface with the bone, especially in studies that are used in studying orthopedic or periodontal implants[21], [93], [94].

2.6 Effect of hyperglycemia on bone cells

2.6.1 Osteoblast proliferation and differentiation

Several studies have reported the effects of hyperglycemia on osteoblasts. The vast majority of these were conducted in the framework of *in-vitro* models for Diabetes Mellitus (DM), a metabolic disorder characterized by hyperglycemia caused by defects in insulin secretion, insulin action, or both[33]–[36]. Untreated DM has been one of the common contradictions in implant therapy[30] as it alters the bone formation and remodelling process and also negatively impacts the wound healing process during osseointegration[30], [95]. The root cause of these effects is the impairment of cellular function observed in osteoblasts under hyperglycemic conditions[96], [97].

Results from *in-vitro* research revealed that even though a change in the morphology of osteoblastic cells was not observed in hyperglycemic conditions[98], their proliferation is negatively impacted. Shao *et al.* reported a decrease in the proliferation of MG-63 cells under high glucose conditions stimulated through high glucose supplement media[94]. A decrease in the proliferation of osteoblasts differentiated from bone marrow-mesenchymal stem cells (MSCs) of diabetic rats compared to healthy rats was also observed by Bueno *et al.* [98]. Valdez-Salas *et al.* also demonstrated an initial decrease in the proliferation of MC3T3E-1 preosteoblasts cultured in human diabetic serum[99].

Similarly, several studies have reported a decrease in the expression of necessary transcription factors that regulate osteoblast differentiation in hyperglycemic conditions. RUNX2, or the Runt-related transcription factor 2, is an important transcription factor that regulates the differentiation of mesenchymal cells into pre-osteoblast and the formation of immature osteoblasts. It is also responsible for inhibiting the differentiation of mesenchymal cells into chondrocytes and adipocytes[100], [101]. However, insulin-deficient animal models have shown that RUNX2 transcripts are lowered in hyperglycemic conditions [102]. RUNX2 expression levels were also lower in osteoblasts differentiated from bone marrow mesenchymal stem cells of diabetic rats[98]. Chen *et al.* also showed similar results, reporting a diminished expression of RUNX2 in rat MSCs in hyperglycemic conditions[103]. In addition, Lu *et al.* also reported a reduced expression and down-regulation of RUNX2 genes in hyperglycemic

mice[104](**Figure 2.2 A**). Liu *et al.* further confirmed the detrimental effects of hyperglycemia by an *in-vitro* analysis of RUNX2 expression in MC3T3E-1 cells grown in media supplemented with various high glucose concentrations[105].

Osteoblast differentiation is also characterized by Alkaline phosphatase (ALP)[106]. ALP is considered to be an early marker of osteoblast differentiation, and an increased ALP level indicates active bone formation since it is a by-product of osteoblast activity[106]. Although, under hyperglycemic conditions, studies analyzing ALP activity have produced contradicting results.

Osteoblasts differentiated from bone marrow MSCs of diabetic rats have shown diminished ALP levels compared to those obtained from healthy rats[98], [103]. However, a long-term assessment by Botolin *et al.* (**Figure 2.2 B**) showed induction of ALP expression in hyperglycemic conditions [107]. Similarly, a higher ALP activity in MC3T3E-1 cells grown in media supplemented with varying high levels of glucose concentrations was observed by Liu *et al.*[105]. Although, the reasons for these contradictions have not yet been established clearly.

Hyperglycemia influences other markers of osteocalcin differentiation, like Osteocalcin (OCN). OCN is a late-stage marker of osteoblastic differentiation produced by mature osteoblasts and is responsible for developing the inorganic matrix of the bone [108]. It is also reported to improve adherence in the case of osteoblast-like cells [109]. However, several studies over the years have reported that a decrease in OCN expression in animal models of hyperglycemia has been observed [104], [107], [110]. Similar decreased expression of OCN was also reported in osteoblasts differentiated from bone marrow MSCs of diabetic rats[98]. *In-vitro* hyperglycemic studies by Shao *et al.* using MG-63 cells also reported a negative OCN expression in high glucose conditions[94](**Figure 2.2 C**).

Additionally, OCN has been shown to have an association with glucose homeostasis. In this regard, a study conducted by Wei *et al.* showed an increase in insulin expression in pancreatic islets cultured with mouse osteoblasts[111]. Furthermore, this rise in insulin expression was not observed in osteoblasts obtained from mice deficient in OCN(OCN-/-). Besides, these mice were found to be hyperglycemic and hypoinsulinemic even with a regular diet. In summary, it was concluded that OCN is a hormone responsible for insulin expression and secreted by osteoblasts which also act as endocrine cells[111]. It was also seen that OCN and insulin are in a regulatory loop monitored by insulin receptors on osteoblasts. These results indicated the importance of OCN in maintaining glucose homeostasis and insulin signalling.[111]

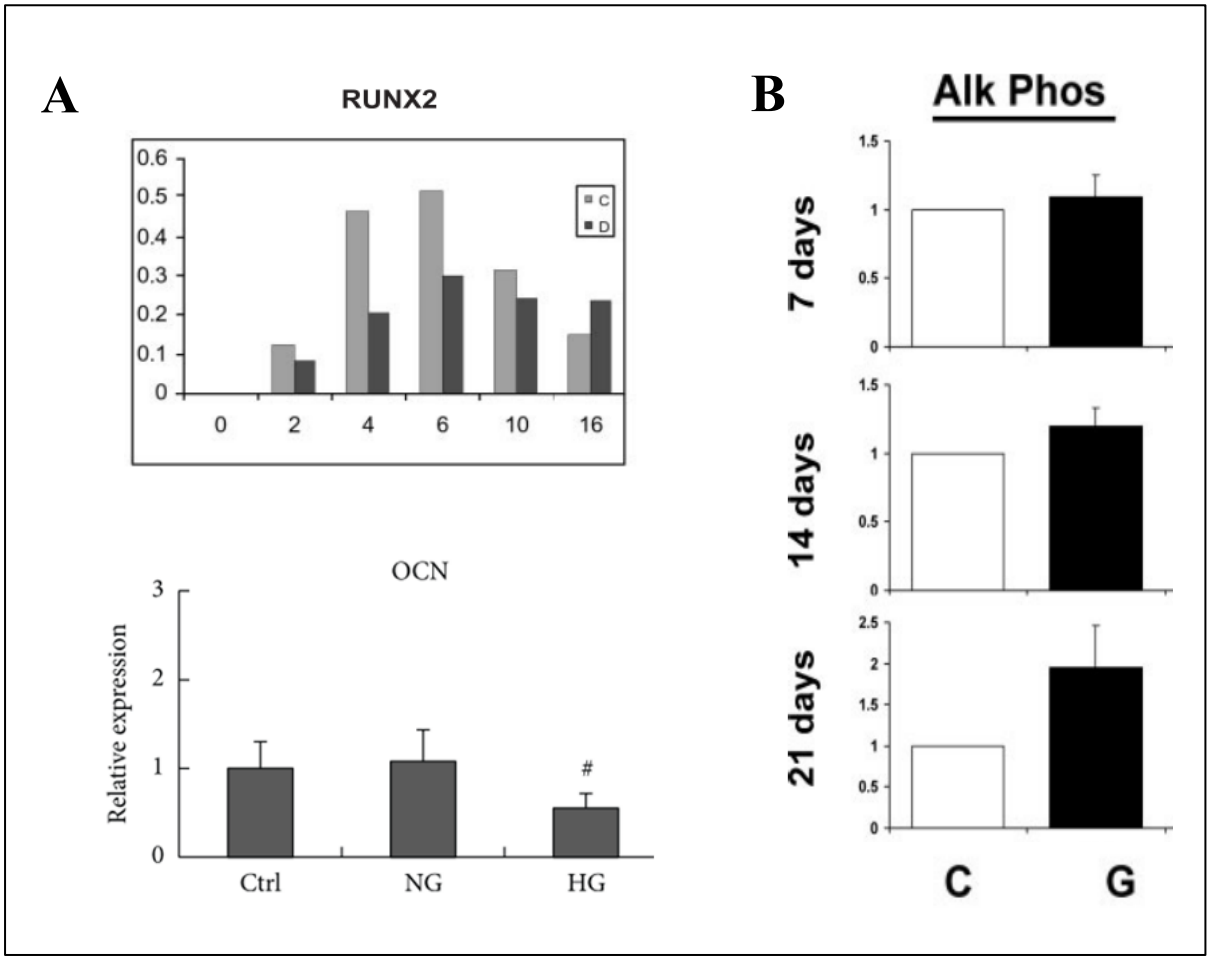

Figure 2.2: Effect of hyperglycemia on osteoblasts

(**A**)RUNX2 expression in control(C) and diabetic mice(G) at different time points(days)[104] *Copyright © 2003 by The Endocrine Society*. (**B**)ALP activity in osteoblasts with treated 30 mM glucose (black bars) and 5.5 mM glucose conditions (control, white bars)[107] *Copyright © 2006 Wiley-Liss, Inc.*. (**C**) OCN expression in MG63 cells under control DMEM (ctrl), normal glucose (NG), high glucose (HG)[94] *Copyright © 2014 Xinyu Shao et al.*.

2.7 Hyperglycemia and surface modifications

Extensive evidence in the previous section indicates that hyperglycemia impairs osteoblast cellular functionality (e.g., proliferation, differentiation, mineralization). Since nanostructured surfaces have been shown to exert favourable effects on osteoblastic functionality, proliferation and osteogenic expression compared to their nonmodified counterparts, current research is focused on understanding whether these surfaces can rescue osteoblastic cells from the detrimental effects of hyperglycemia.

In this context, Jiang *et al*. reported that sandblasted/acid-etched and anodized titanium surfaces improved the proliferation and differentiation of MC3T3-E1 osteoblast cells in high glucose concentrations (25 mM)[70]. Similarly, Valdez-Salas *et al*. showed that nanostructured TiO_2 nanotubes upregulated osteoblastic differentiation in MC3T3-E1 osteoblast cells under high glucose conditions stimulated by human diabetic serum [99]. Moreover, Yang *et al.* also reported that TiO_2 nanotubes supported osteoblastic proliferation and differentiation in high glucose concentrations(22 mM)[112]. However, despite these results, the mechanisms of how nanostructured surfaces affect cells are not fully elucidated.

This study will thereby contribute to the body of literature that uses high glucose content to mimic the osseointegration of biomaterials in diabetic conditions by utilizing oxidative nanopatterning to understand further and decipher the role that nanoporous titanium plays in rescuing osteoblast from the adverse effects of hyperglycemia.

Chapter 3

MATERIALS AND METHODS

3.1 Surface Preparation

3.1.1 Titanium substrates

Grade 2 titanium squares (1cm X 1cm, 1 mm in thickness) were obtained from a 200 X 200 mm Titanium foil (99.2% (metals basis), Thermo Scientific). The samples were cut using the electronic discharge machine and were cleaned in toluene in an ultrasonic bath for 20 mins, followed by ultrasonic rinsing in deionized water (DI) three times. A portion of these samples was kept as the **Control (Ti)** condition. 12mm borosilicate glass coverslips (#1.5, Fisher, 1254580), referred to as **CS,** were also ultrasonically cleaned with toluene and rinsed three times in DI.

3.1.2 Oxidative nanopatterning

Samples were treated with the "Piranha Solution," which was prepared as a 1:1 mixture of H_2SO_4 (37N, Fisher Scientific) and H_2O_2 (30%, Fisher Scientific). The solution was cooled down by placing it in an ice bath until it reached room temperature. Successively, samples were carefully placed along the edge of the beaker, and the solution was stirred using a magnetic stirrer for a period of 2 hours, according to a previously established protocol[37]. After the treatment, the samples were rinsed three times in DI and successively air-dried. These treated samples were labelled as **Nanoporous Titanium (NPTi)**.

3.2 Surface Characterisation

3.2.1 Scanning electron Microscopy (SEM)

SEM imaging was carried out with JSM-7500F Field Emission Scanning Electron Microscope (FESEM, JOEL, Japan). The primary purpose was to ensure that the chemical treatment created the characteristic nanoporous surfaces on titanium previously reported in the literature [9], [27], [28], [37].

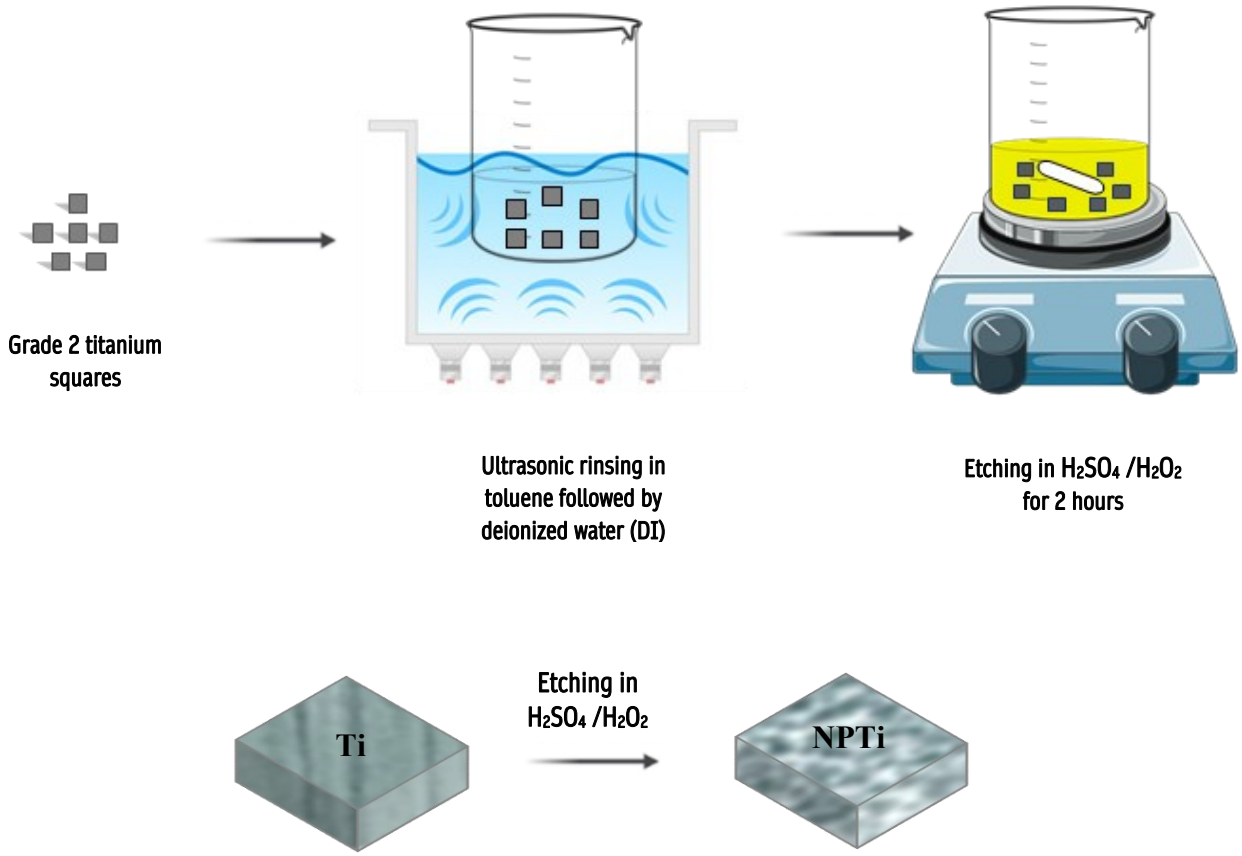

Figure 3.1: Schematics of sample preparation

Sample preparation to produce Control Untreated Titanium (Ti), Nanoporous Titanium (NPTi) conditions.

3.3 Cell culture

Aliquots of commercially available human osteoblastic MG-63 cells (ATCC, USA) kept in the -80 °C freezer were thawed in a 37 °C water bath. The 1 mL volume contained in the vial was gently transferred to a 15 mL centrifuge tube using a 1 mL pipette. Successively, 9 mL of pre-warmed cell culture medium (DMEM + 1g/L glucose supplemented with 10% Fetal bovine serum (FBS), 20 U mL^{-1}penicillin and 20 U mL^{-1}streptomycin (ThermoFisher Scientific, USA) and 1% L-glutamine (ThermoFisher Scientific, USA) at 37° C was added to make a cell suspension of 10 mL. The cell culture medium was added to the 15 mL tube in a dropwise fashion while rotating the tube by hand to prevent osmotic shock. The cell suspension was centrifuged at 190 g for 6 minutes. The pellet was resuspended in a 10 mL cell culture medium, transferred to a fresh 75 cm^2 cell culture flask, and placed at 37 °C in a water-jacketed incubator with 5% CO_2 / 95% air atmosphere and at 100% humidity.

Cells were grown in Dulbecco's modified eagle medium, with different glucose levels, normal glucose (5mmol/L or 1g/L glucose) and high glucose (25 mmol/L of 4.5g/L glucose) at 37 °C in a water-jacketed incubator with 5% CO_2 / 95% air atmosphere and at 100% humidity. The media was changed every two days. Cells were trypsinized when they reached a 70-80% confluency. Once confluent, cells were detached from the surfaces using appropriate volumes of 0.25% trypsin-EDTA and incubating at 37 °C for 5 minutes. To ensure the complete neutralization of the trypsin enzyme equal volume of appropriate pre-warmed fresh culture media was added, followed by throughout mixing. Cells were collected and centrifuged at 190 g for 8 mins, the supernatant discarded, and the pellet reconstituted in appropriate (normal glucose or high glucose) pre-warmed fresh culture media to desired concentrations specific to the experiment, approximately $2x10^4$ cells per mL.

Cells were grown in normal and high-glucose cell culture medium to pre-condition them for a period of 14 days before seeding them onto the samples.

3.4 Cell seeding

Both Ti and NPTi samples were sterilized with 70% ethanol for one hour. Successively, they were washed thrice with 1X phosphate-buffered saline (PBS, GIBCO), 5 minutes each before commencing seeding. The MG-63 cells were seeded in a 24-well plate and 500 mL cell suspension at a concentration of $1x10^4$ cells per sample. Three conditions were used Ti, NPTi and CS as control. The medium was changed in the wells on every alternate date. The samples were seeded separately for high glucose cell culture medium and normal glucose cell culture medium. The plates were cultured for 1 and 3 days for cell morphology analysis, for 1, 3 and

7 days for cell proliferation assays and for 7, 14 and 21 days to assess differentiation. Each experiment was performed in quadruplicates with at least three samples per experimental condition (high or normal glucose).

3.5 Immunofluorescence

Immunofluorescence was used to understand cellular activity and subcellular localization of proteins with specificity and sensitivity. It is a widely employed technique to study cell proliferation and differentiation in surface modification studies[26], [89], [99], [113], [114]. After days 1 and 3 (for Ki-67, Section 3.5.1) and 7 days (for OCN and RUNX2, Section 3.5.2), cells cultured on the titanium samples were carefully washed twice with 1X PBS, 5 minutes each. Cells were successively fixed onto the samples by adding 500 mL of 4%-paraformaldehyde (PFA, pH 7.2) for a period of 15 minutes at room temperature. Following this, the samples were washed thrice with 1XPBS, 5 minutes each. The cells were subsequently permeabilized using 0.5% Triton X-100 for a period of 30 mins. The samples were then washed thrice with 1X PBS, 5 minutes each. A 5% skim milk solution in 1X PBS was prepared using skim milk powder as the blocking buffer. 500 µL of the blocking buffer was added to each well for 30-60 minutes, following which they were washed twice with 1X PBS, 5 minutes each. The samples were then treated with respective antibodies (refer section 3.5.1 and 3.5.2) for analysis.

3.5.1 Ki-67 analysis

The study utilizes the Ki-67 protein, which is recognized as an eminent proliferation marker in pathology[115]–[118]. It is present in the nuclei during the G1, S and G2 phases of cell cycle division and mitosis and not expressed in the G0 phase of resting or quiescent cells[115]. The fact that Ki-67 is absent in resting cells and its expression in proliferating cells[118] led to Ki-67 labelling index via immunofluorescence[115], [116] which has also been employed in previous studies to assess cell proliferation on oxidative nanopatterned titanium and MG-63 cells[15], [119].

To visualize the Ki-67 protein, samples were exposed to primary polyclonal rabbit antihuman Ki-67 oncoprotein (Sigma, SAB4501880-100UG). The antibody was diluted in the appropriate amount of blocking buffer at a dilution of 1:100, which was the best-optimized concentration after dilution experiments. Samples were carefully inverted on a 30 µL droplet of an optimized amount of the primary antibody solution placed on a dish lined with paraffin. The samples were incubated overnight at 4 °C. After incubation, the primary antibody was washed twice with 1X

PBS, 5 minutes each. The secondary antibody, donkey anti-rabbit IgG, was conjugated with Alexa Flour 647 (ThermoFisher, A31573) at an optimized concentration of 1:500 after dilution experiments. 4', 6-Diamidino-2Phenylindole, Dihydrochloride (DAPI; ThermoFisher, D1306), was used for nuclei staining at an optimized concentration of 1:1000 and the actin cytoskeleton was stained using donkey anti-mouse IgG conjugated with Alexa Flour 594 (ThermoFisher, A21203) at an optimized concentration of 1:500. The secondary antibody (Alexa flour 674) along with DAPI and Alexa flour 594 were diluted in appropriated concentration in blocking buffer. The samples were carefully inverted on a 30 µL droplet of an optimized amount of this solution placed on a dish lined with paraffin. The samples were incubated at 37 °C for 1 hour in the dark. The samples were mounted on coverglass (#1.5, VWR 14150626) using Vectashield mounting media (Fisher Scientific, NC9532821).
The process was repeated for both high and normal glucose conditions.

3.5.2 Osteocalcin and RUNX2

To visualize OCN and RUNX2, markers of osteogenic differentiation[85][97], samples were exposed to primary monoclonal mouse antihuman osteocalcin protein (ThermoFisher, 335400) and recombinant monoclonal mouse antihuman RUNX2 protein (ThermoFisher, MA5-41185). The antibody was diluted in an appropriate amount of blocking buffer at a dilution of 1:100 for RUNX2 and 1:200 for OCN, which was the best-optimized concentration after dilution experiments. The samples were carefully inverted on a 30 µL droplet of an optimized amount of the primary antibody solution placed on a dish lined with paraffin. The samples were incubated overnight at 4°C. After incubation, the primary antibody was washed twice with 1X PBS, 5 minutes each. The secondary antibodies, donkey anti-rabbit IgG conjugated with Alexa Flour 647 (ThermoFisher, A31573) and anti-mouse IgG conjugated with Alexa Flour 594 (ThermoFisher, A21203) at an optimized concentration of 1:500 after dilution experiments were used. 4', 6-Diamidino-2Phenylindole, Dihydrochloride (DAPI; ThermoFisher, D1306) was used for nuclei staining at an optimized concentration of 1:1000, and the actin cytoskeleton was stained using donkey anti-goat IgG conjugated with Alexa Flour 488 (ThermoFisher, A21203) at an optimized concentration of 1:500. The secondary antibodies along with DAPI and Alexa flour 488 were diluted in appropriated concentration in blocking buffer. The samples were carefully inverted on a 30 µL droplet of an optimized amount of this solution placed on a dish lined with paraffin. The samples were carefully inverted on a 30 µL droplet of an optimized amount of this solution placed on a dish lined with paraffin. The samples were

incubated at 37 °C for 1 hour in the dark. The samples were mounted on coverglass (#1.5, VWR 14150626) using Vectashield mounting media (Fisher Scientific, NC9532821).
The process was repeated for both high and normal glucose conditions.

3.5.3 Image Acquisition

The mounted samples were imaged using the AxioOserver 7 inverted microscope (Zeiss, Germany). Multi-channel images were captured using different filter sets; Filter Set 37 (DAPI), Filter Set 43 HE (Phalloidin), and Filter Set 50 (Ki-67). Using the 10x, 0.3NA EC Plan-NeoFluar objective, the samples were observed at low magnification. A total of 25 images per sample were captured using the 5X5 tiles features using the 20X, 0.8NA Plan-Apochromat objective for assessment of general morphology, cell proliferation and differentiation. High magnification 5X5 tiled images imaged with 40x, 1.3NA, Oil, Fluar objective were used for high-resolution cell structure images.

3.6 Image analysis

The acquired images were quantitatively analyzed after stitching and focus stacking, and deconvoluting them in AxioVision Mosaix Software (Zeiss).

3.6.1 Cell morphology

The cell morphology was measured using CellProfiler, cell image analysis software, version 4.2.5. Custom pipelines were created in CellProlifer that were rigorously and periodically calibrated for the images to maintain quality results. The main measurements that were scrutinized for the cell structure were cell perimeter, area, compactness, and form factor. The cell area was determined by counting the number of pixels within the identified cells. The measure of the number of pixels around the boundary of the identified cell periphery was determined as the perimeter. The form factor reveals the cell shape irregularity. And it is measured using the following equation.

$$F = \frac{4 * \pi * A}{P^2}$$

Where A is the area and P is the perimeter. A calculated value of 1 was associated with perfectly circular objects. The measure of the deviation of the cell from circularity was assessed using eccentricity, which is calculated as the ratio of the distance between the foci of the ellipse and

its major axis length. It has a value between 0 and 1, a 0 eccentricity value means that the ellipse is a circle, and 1 means it is a line segment.

3.6.2 Ki-67 index

The proliferation of the cells was determined using the Ki-67 index. The processed images were analyzed using IMARIS, an interactive microscopy image analysis software. Using custom pipelines, which were rigorously calibrated, the number of positive Ki-67 cells and the total number of cells were determined. The Ki-67 index percentage was obtained using the following formula.

$$Ki\text{-}67\ index = \frac{Number\ of\ positively\ stained\ cells}{Total\ number\ of\ cells}\ X\ 100$$

3.8 Presto Blue Assay

PrestoBlue assay was used because it is a non-destructive cell viability assay containing a growth indicator which is reduced by metabolically active cells to a fluorescent agent, which allowed us to monitor the trend of cell proliferation for 7 days, unlike end-point analysis; which would not be pertinent in this study[122], [123].

At 1, 3 and 7 days, 10% Presto Blue reagent (ThermoFisher Scientific, USA) in the appropriate cell culture medium was added to each well at a volume of 500 µL per well. The PrestoBlue solution was also added directly to the cell culture plate which was used as blank control. The plates were incubated at 37 °C in the incubator for an optimized reaction time of 1 hour. The Presto blue solution was then added to a 96-well plate at 100 µL per well. The fluorescence intensity was measured at 560 and 590 nm using a plate reader. The exact process was repeated for both high and normal glucose conditions.

3.9 Alkaline Phosphate Assay

To estimate cellular ALP activity in the cell lysate, at days 7, 14 and 21, the conversion of p-nitrophenyl phosphate (pNPP) to p-nitrophenol (pNP) was measured. The pNPP tablets (ThermoFisher Scientific, USA) were equilibrated to room temperature and added to readily purchased Diethanolamine Substrate Buffer (ThermoFisher Scientific, USA) diluted from 5X to 1X concentration. 10 mg of pNPP (two pNPP tablets) was dissolved in 10 mL of 1X Diethanolamine Substrate Buffer. The solution was vortexed for a couple of minutes to ensure

that the tablets dissolved entirely in the buffer. 500 µL of this solution was added to each well containing the samples. The pNPP solution was also added directly to the cell culture plate which was used as blank control. The plates were incubated for 90 minutes, which was the optimized reaction time for sufficient development of the colour. 250 µL of 2N NaOH (Sigma) was added to each well to stop the reaction. The amount of pNP was estimated by transferring 100 µL from each sample solution into 96-well plates and measuring the absorbance at 405 nm using a plate reader. The exact process was repeated for both high and normal glucose conditions.

3.10 Western Blot

After 7 days, the cell culture plates were placed on ice, and 2X Laemmli buffer (10µL per well per sample) was placed on the samples (Ti, NPTi and CS); the surface was scratched using a cold plastic cell scraper to remove the adherent cells, and the harvested protein was gently transferred into a microcentrifuge tube. The cell lysate was boiled at 90 °C for 10 mins. SDS Page gel was prepared by using BioRad TGX Stain-Free FastCast 10% acrylamide kit. The resolver solution was added between the glass plates, and after it was set, it was followed by the stacker gel solution. Protein solutions were loaded into each well along with a molecular weight ladder (Pre-stained protein ladder; ThermoFisher Scientific, USA). The gel was run at 50 V for 5 mins, after which the voltage was increased to 150 V till the run was finished. The gel was placed in a 1X transfer buffer for 5 minutes. The nitrocellulose membrane was activated by placing it in methanol for one minute. The semi-dry transfer sandwich was assembled with extra-thick blotting filter papers, ensuring that no air bubbles were trapped between the layers. The transfer was run for 20 mins at 20V in BioRad Trans-Blot® SD semi-dry transfer cell. The blotted membrane was washed with Tris-buffered saline with Tween 20 (TBST) buffer before it was blocked with 5% bovine serum albumin (BSA) in TBST for 1 hour on a shaker at a slow speed. The primary antibody for RUNX2 (Thermo Fisher Rabbit anti-RUNX2, MA541185) was diluted in blocking buffer at a concentration of 1:1000, and the blot was incubated overnight in this solution at 4 ºC. The membrane was then washed thrice in TBST, 5min each and incubated in the horseradish peroxidase-conjugated secondary antibody (Life Technologies, Goat anti-Rabbit IgG-HRP, G21234) diluted 1:5000 in blocking buffer. Bands were imaged with Bio-Rad, Chemidoc MP. The same procedure was repeated for determining OCN differentiation, with the primary antibody for OCN (Thermo Fisher Mouse anti-

Osteocalcin, 335400) and horseradish peroxidase-conjugated secondary antibody (Thermo Fischer Scientific, Goat anti-mouse IgG-HRP,62-6520). The process was repeated for both high and normal glucose conditions.

3.11 Statistical Analysis

The experimental data are evaluated by analyzing the significant differences from at least four independent experiments, each in quintuplicate.

Statistical analysis was performed using one-way analysis of variance (ANOVA) followed by Tukey's multiple comparison test for multiple group comparisons using GraphPad Prism 7.0. The data from the experiments are represented as the mean and the standard deviation of the mean (mean ± standard deviation (SD)). The significant differences are represented by asterisks (* = $p < 0.05$, ** = $p < 0.01$, ***$p < 0.0005$, ****$p < <0.0001$).

Chapter 4

RESULTS and DISCUSSION

4.1 Material Characterisation

4.1.1 SEM Analysis

In order to identify the topographical characteristics of nanoporous surfaces, SEM imaging was used to visualize the surface nanoscale changes that occurred due to the oxidative nanopatterning of titanium. SEM micrographs (**Figure 4.1 B-C**) revealed that **Ti** controls did not display any topographical features at the nanoscale, aside from irregular elements which resulted from the mechanical polishing of the original foil. Conversely, **NPTi** displayed the characteristic 3-dimensional network of nanopits, as expected based on published literature[4], [9], [15], [28], [37]. Image analysis of SEM micrographs revealed a non-uniform size distribution of nanopits with an average nanopore diameter of 21 ± 8 nm, which confirmed earlier studies [37]. The histogram in **Figure 4.1 A** was determined by analyzing a total number of 40 nanopits throughout 4 independent experiments with 10 nanopits each (n=4). From a qualitative standpoint, it is evident that the chemical treatment modifies the nanotopography of titanium, as can be clearly observed from **Figure 4.1 B-C**. Taken together, these findings reiterate the high degree of reproducibility offered by oxidative nanopatterning, thereby vouching for the consistency of the protocol and, ultimately, for its application in interfacial studies aimed at investigating the interplay between cells and nanoengineered surfaces.

4.2 Bioactivity of MG-63 cells

To assess the biological response to nanoporous titanium, we carried out cell culture studies with MG-63 human osteoblastic cells. This cell line was chosen as it has been proven to be a better model to adopt given its fibroblast-like morphology, which therefore makes them more suitable for fluorescence imaging when compared to other human osteoblastic cells, such as Saos-2 [91]. Notably, MG-63 cells have been previously used in fundamental studies aimed at assessing the role of hyperglycemia in the osteoblastic response[94], thereby providing an important benchmark to compare our results.

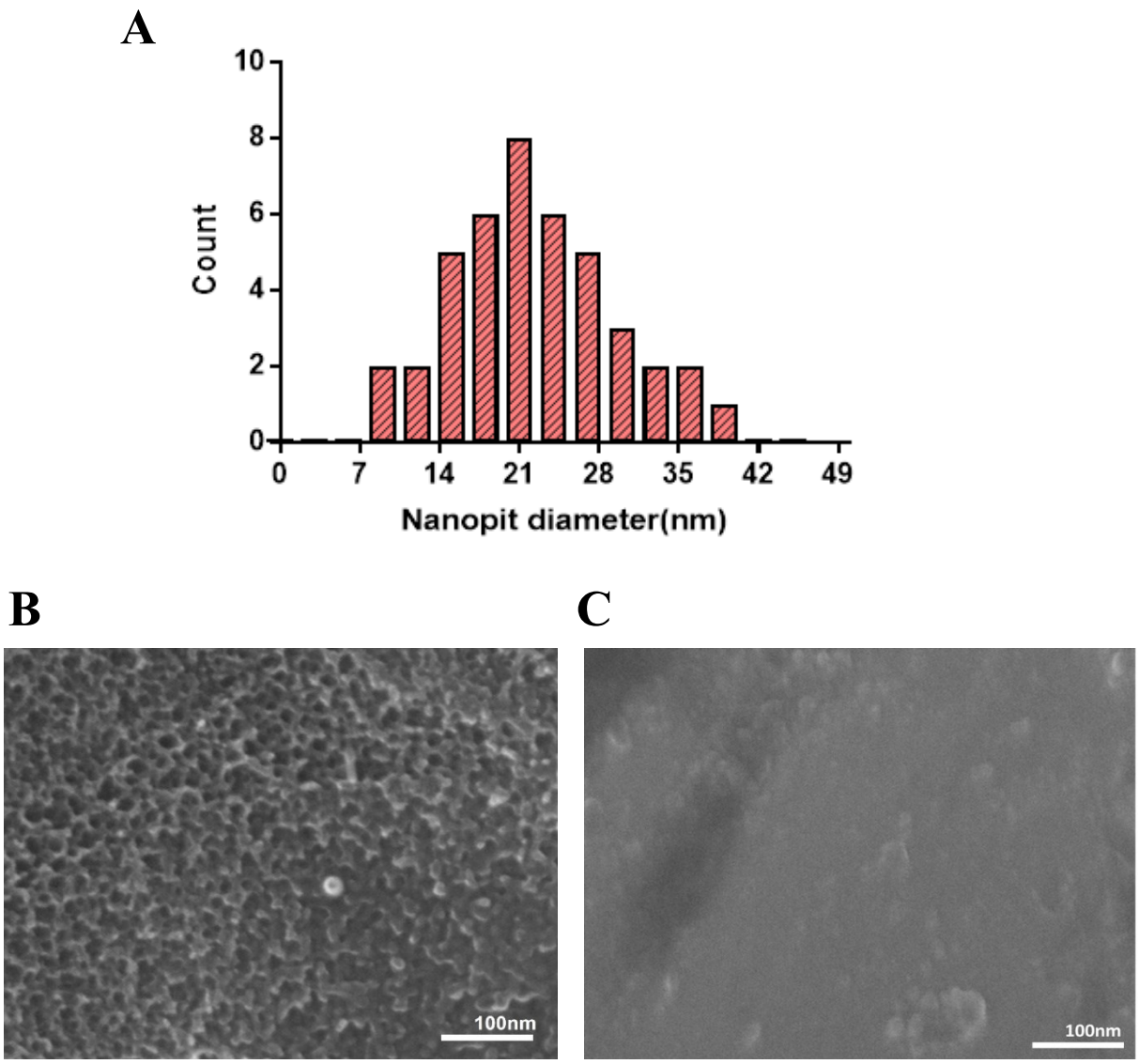

Figure 4.1: SEM imaging and nanopit diameter

(A) Size distribution **(B)** SEM image of NPTi **(C)** SEM image of Ti, *Scale bar=100µm*

4.2.1 Morphological Analysis

To investigate the impact exerted by oxidative nanopatterning of titanium at the single-cell level, I first carried out a qualitative analysis based on fluorescent imaging. Representative images of MG-63 cells adhering on both control and nanoporous titanium (**Figures 4.2 and 4.3**) exhibited a large and elongated morphology with membrane projections (i.e., lamellipodia and filopodia). From the qualitative analysis, it became evident that no discernible morphological differences existed between Ti and NPTi samples in both normal and hyperglycemic conditions after 1 and 3 days of culture.

To further close in on our understanding of substrate-driven morphological alterations, I proceeded to quantify substrate-dependent variations in cell morphology in terms of aspect ratio(i.e. minimum diameter/maximum diameter, determines cell interspersion during division)[124], form factor (calculated as $4\pi X area/perimeter^2$, determines the shape of the cell)[125], eccentricity (a measure of the deviation of cell from circularity)[126] and area (spreading(a sign of adherence to the substrate))[127]. **Figure 4.4** shows these parameters after 1 and 3 days of culture, determined by analyzing data collected from a total number of 160 samples during 4 independent experiments with 20 different samples for each condition and timepoint (n=4). **Figures 4.4 A** and **E** confirm the qualitative observations, namely that elongated shape characterization is observed in both cells adhering to Ti and NPTi samples, also presenting that this morphology is adapted early on. Comparison of the form factor in **Figure 4.4 B** and **F** provides information about the cell shape complexity (i.e., jagged edges). As expected from the qualitative observation, cells adhering onto both NPTi and Ti samples showed a similar elongated morphology. A similar trend was also determined for the eccentricity and aspect ratio: **Figure 4.4 C** and **G** display a similar degree of cell elongation for all conditions tested.

However, a significantly larger (35-50%) surface area of cells in contact with NPTi samples at Day 3 was seen compared to Ti samples regardless of glucose levels (**Figure 4.4 D** and **H**), demonstrating a higher cell spreading on treated samples at longer culturing intervals. These observations are indicative of the enhanced bioactivity exerted by nanoporous titanium. The similar morphology, regardless of glucose levels, could be attributed to the pre-conditioning step. In fact, no morphological differences between cells grown in normal and hyperglycemic conditions have been previously observed in osteoblasts obtained from healthy and diabetic animals or patients[98].

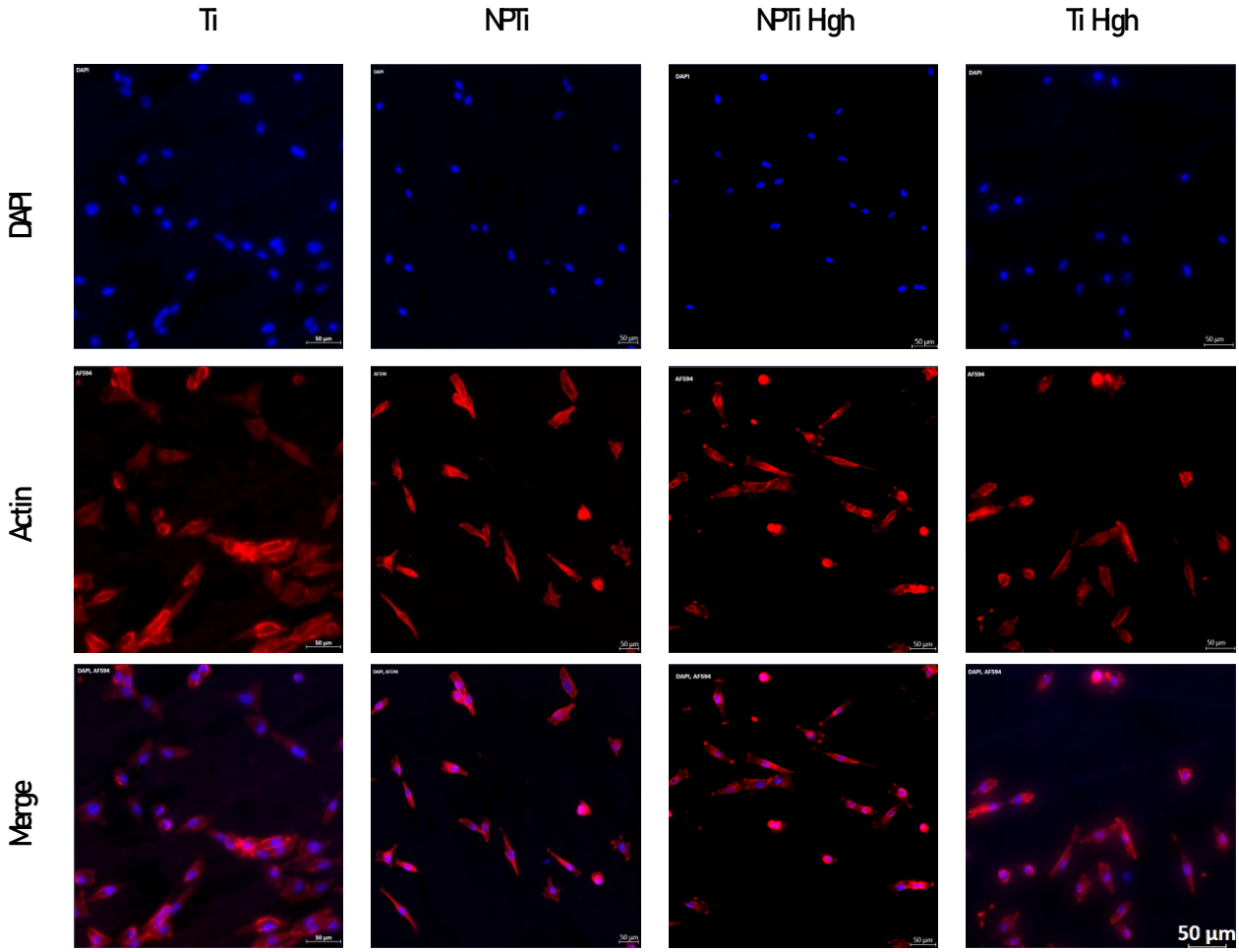

Figure 4.2: Immunofluorescence images of MG-63 morphology at day 1

Representative images of immunofluorescence staining, blue (DAPI) and red (Actin), *Scale bar=50µm;* Ti: Control titanium in normal glucose conditions, NPTi: Nanoporous titanium in normal glucose conditions, Ti High: Control titanium in high glucose conditions, NPTi High: Nanoporous titanium in high glucose conditions.

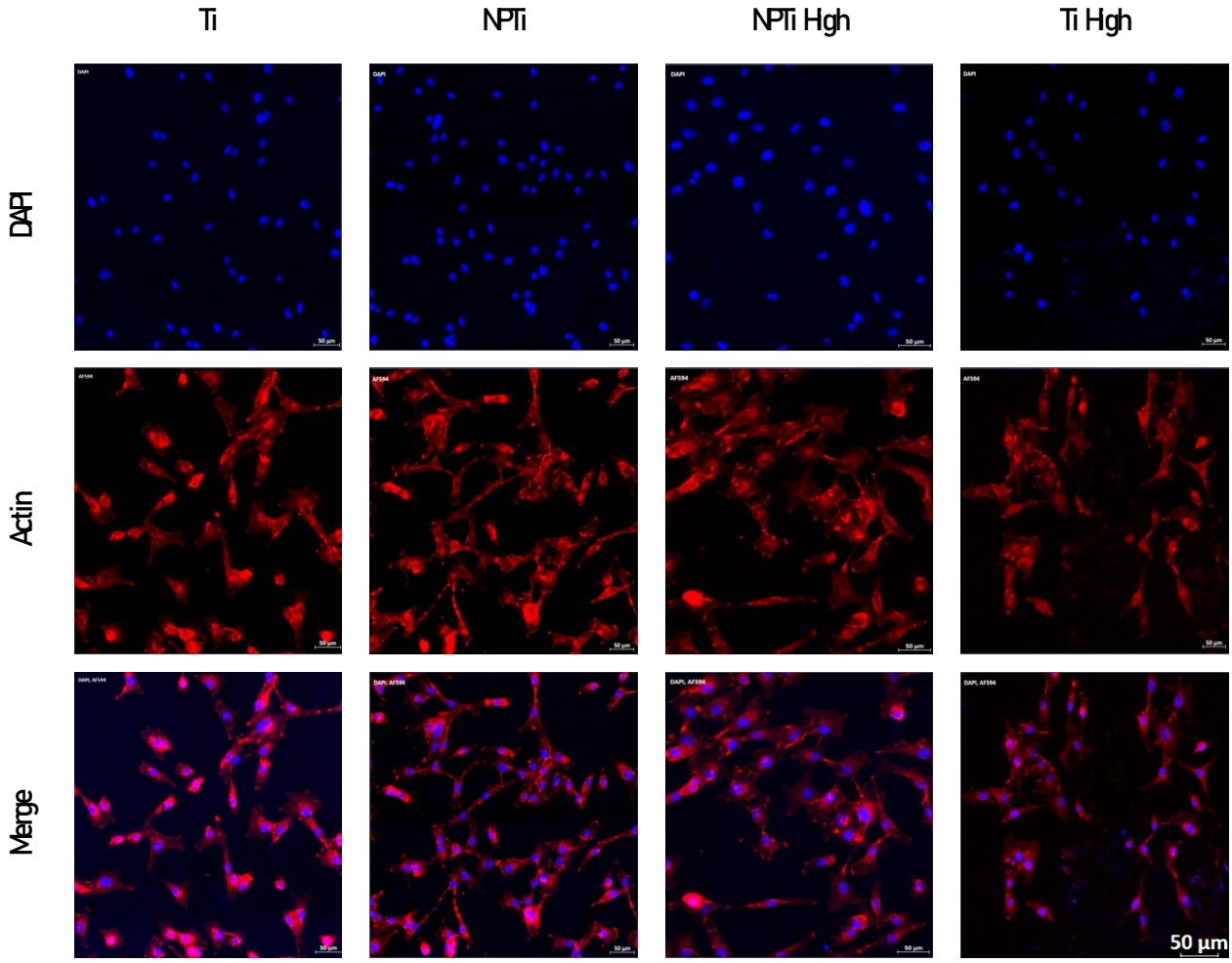

Figure 4.3: Immunofluorescence images of MG-63 morphology at day 3

Representative images of immunofluorescence staining, blue (DAPI) and red (Actin), *Scale bar=50µm;* Ti: Control titanium in normal glucose conditions, NPTi: Nanoporous titanium in normal glucose conditions, Ti High: Control titanium in high glucose conditions, NPTi High: Nanoporous titanium in high glucose conditions.

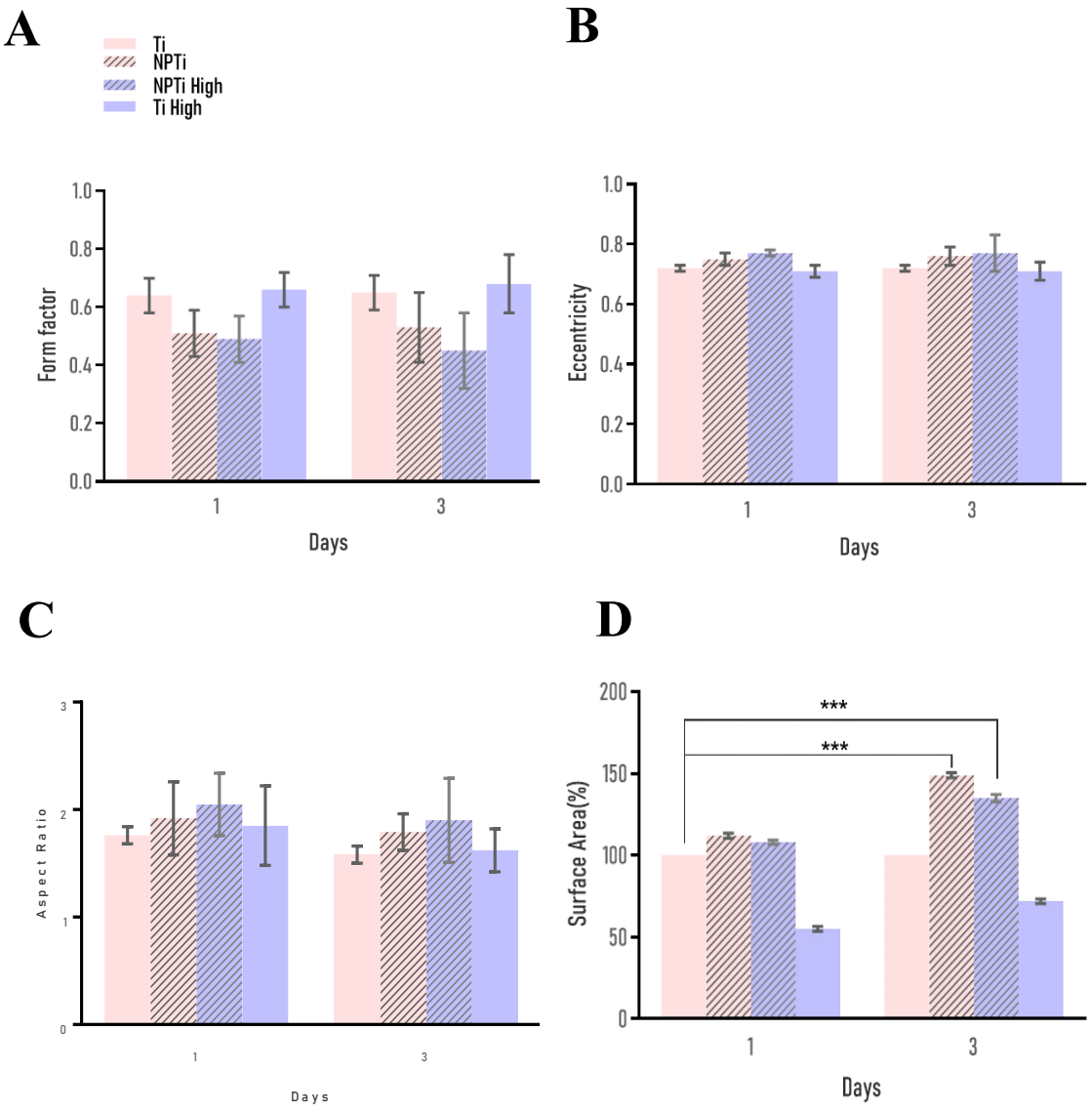

Figure 4.4: Cell spreading and Morphology

(A)Form factor, (B) Eccentricity, (C) Aspect Ratio and (D) Surface contact area (expressed as percentage increase/decrease in respect to bare titanium) of MG-63 osteoblastic cells at Day 1 and Day 3. (ANOVA test, (n=4): ***p< 0.0005)

I thus believe that pre-conditioning MG-63 cells allowed us to create a cellular environment similar to that present in diabetic mouse models characterized by higher levels of glucose. Although further studies are required to confirm this hypothesis.

4.2.2 Proliferation Analysis

In these experiments, I evaluated the proliferation of MG63 cells using two different approaches, namely Ki-67 analysis and PrestoBlue assay, which are both well-established methods to assess cell proliferation[115]–[118], [123]. The experiments were performed at short (Days 1 and 3) and longer intervals (Day 7) to validate the effects of oxidative nanopatterning on the capacity of cells to grow and proliferate. The question now is to determine whether the nanoporosity can compensate the well-known detrimental effects of hyperglycemia on MG-63 proliferation[94]. **Figures 4.5 and 4.6** display the representative images of Ki-67 expression in MG63 cells at day 1 and day 3. **Figure 4.7** displays the relative variations in cell proliferation at days 1 and 3 determined by employing the IMARIS software to count nuclei expressing the Ki-67 protein, an eminent proliferation indicator[115]–[118] that was determined by analyzing data collected from a total number of 160 samples, during 4 independent experiments with 20 samples in each experimental condition and timepoint (n=4). My results demonstrated that cell proliferation did not significantly vary in relation to the substrate at day 1. However, a higher cell count was observed on Ti and NPTi substrates in normal glucose condition samples in comparison to the hyperglycemic state, although the difference was not statistically significant. While cell proliferation was not expected to be a predominant effect at this early stage, the overall decrease in cell count observed on samples in high glucose conditions could be indicative of the detrimental effects of hyperglycemia on cell viability[96]. A remarkable increase in proliferation was, however, observed on day 3; the proliferation of cells grown on NPTi samples experienced a statistically significant ($p < 0.01$) increase of around 65-70% with respect to Ti samples in normal glucose levels, which is evidence of enhanced bioactivity exerted by oxidative nanopatterning. An increase was also observed in cell proliferation on NPTi samples with respect to Ti samples in high glucose, although the findings were not statistically significant. These findings confirm previous studies which showed the ability of oxidative nanopatterning of titanium to enhance cell proliferation in different cell lines, ranging from primary osteoblasts to stem cells[4], [25], [27].

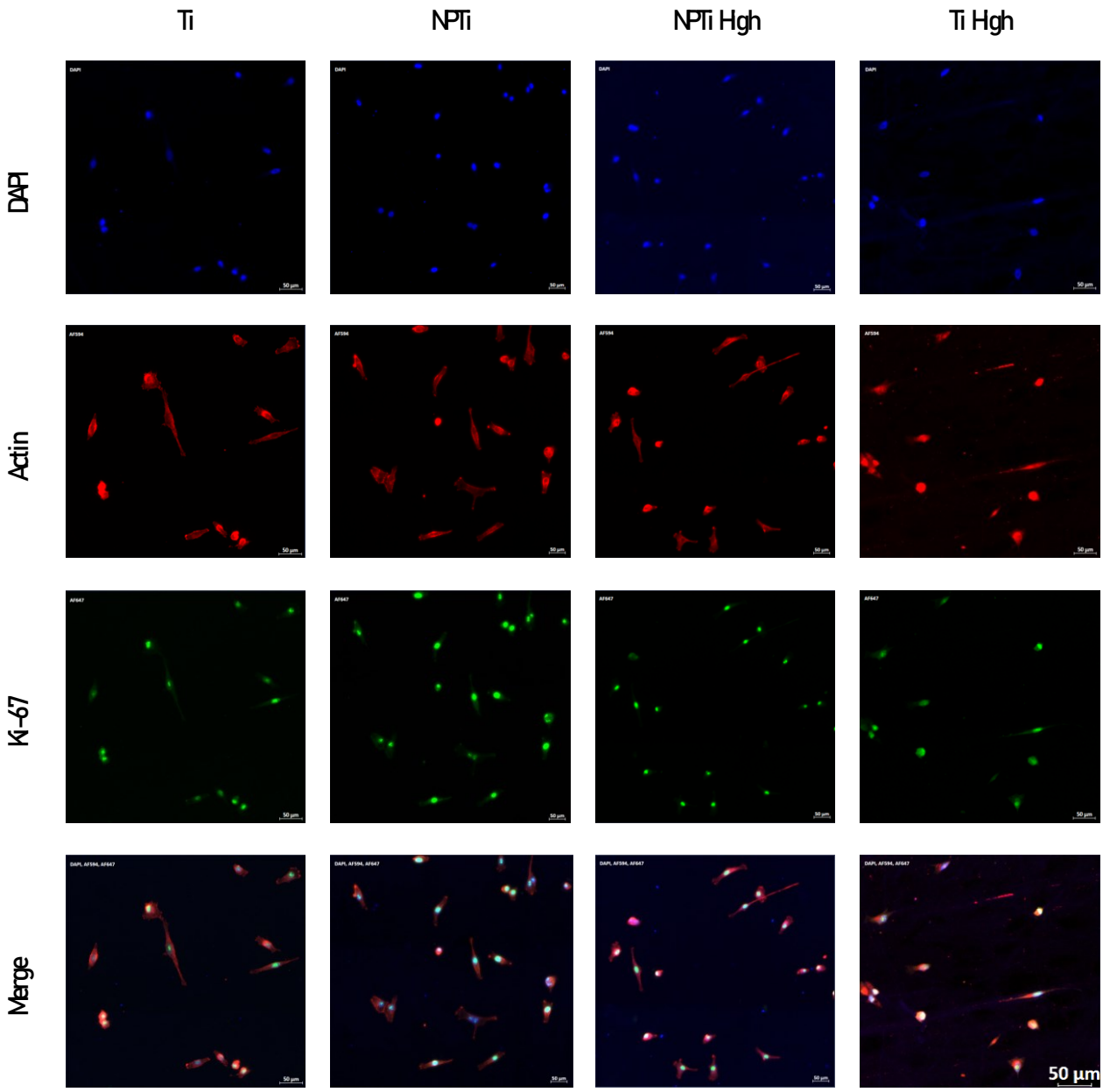

Figure 4.5: Immunofluorescence images of Ki-67 expression at day 1

Representative images of immunofluorescence staining, blue (DAPI), red (Actin), green (Ki-67), *Scale bar=50µm*; Ti: Control titanium in normal glucose conditions, NPTi: Nanoporous titanium in normal glucose conditions, Ti High: Control titanium in high glucose conditions, NPTi High: Nanoporous titanium in high glucose conditions.

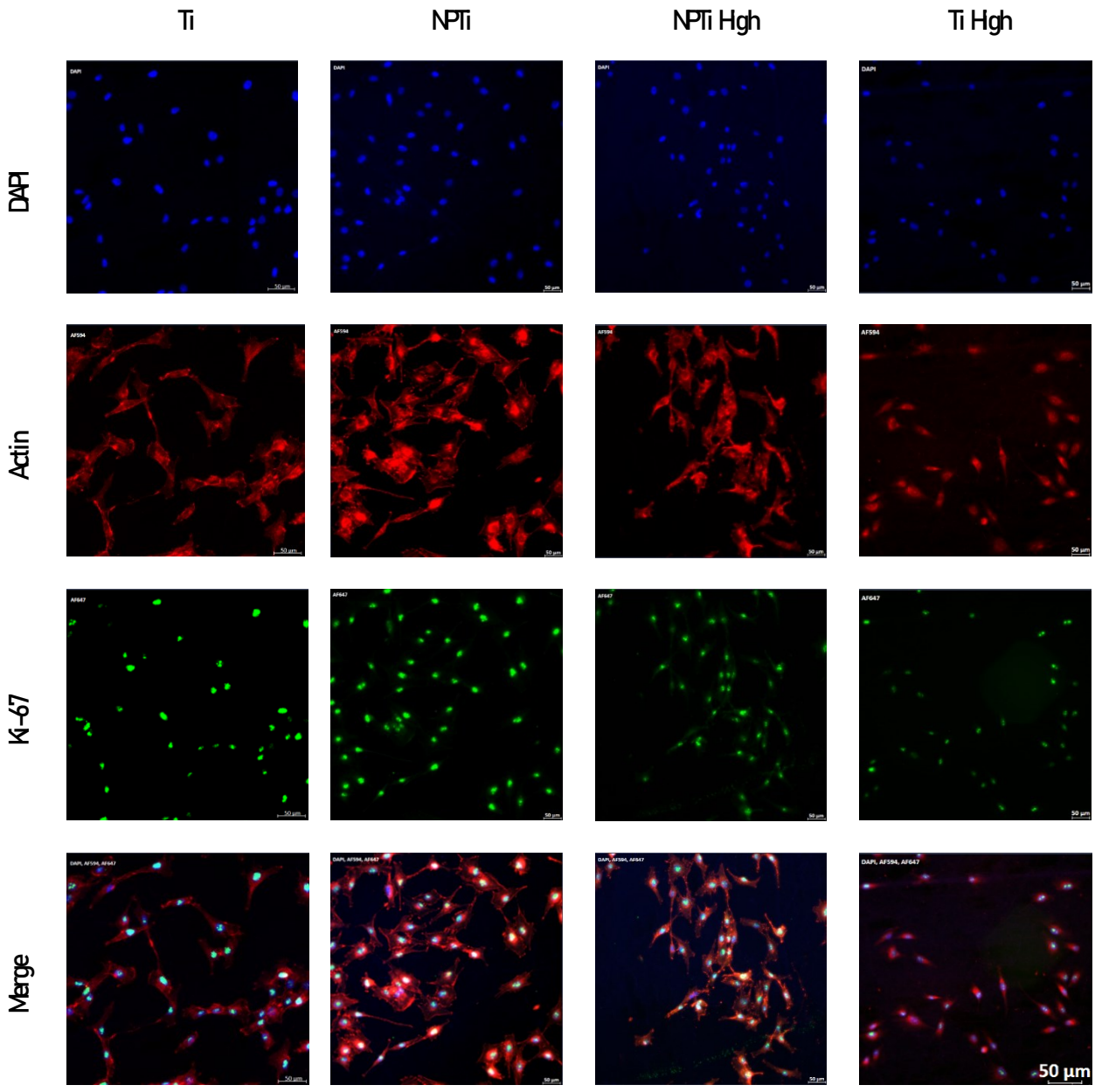

Figure 4.6: Immunofluorescence images of Ki-67 expression at day 3

Representative images of immunofluorescence staining, blue (DAPI), red (Actin), green (Ki-67), *Scale bar=50µm;* Ti: Control titanium in normal glucose conditions, NPTi: Nanoporous titanium in normal glucose conditions, Ti High: Control titanium in high glucose conditions, NPTi High: Nanoporous titanium in high glucose conditions.

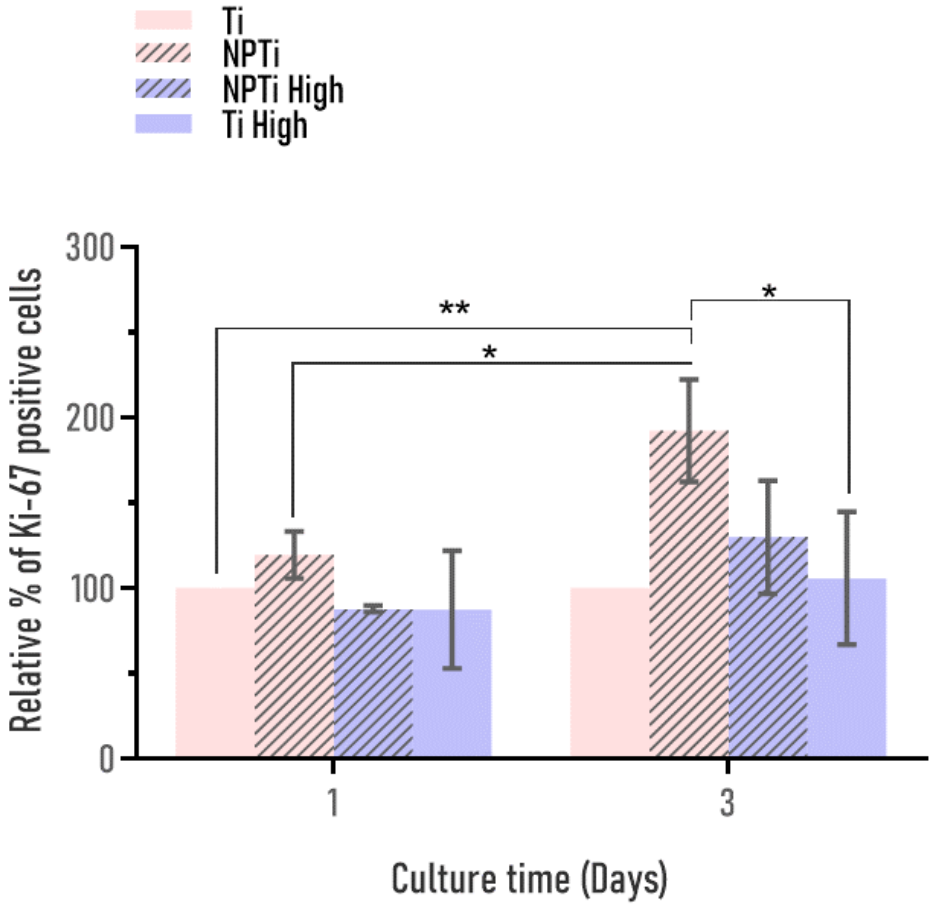

Figure 4.7: MG-63 cell proliferation by Ki-67 analysis

Ki-67 index on Day 1 and 3. (ANOVA test, (n=4): * = $p < 0.05$, ** = $p < 0.01$). Results are expressed as percentage increase/decrease with respect to bare titanium in normal glucose levels (Ti).

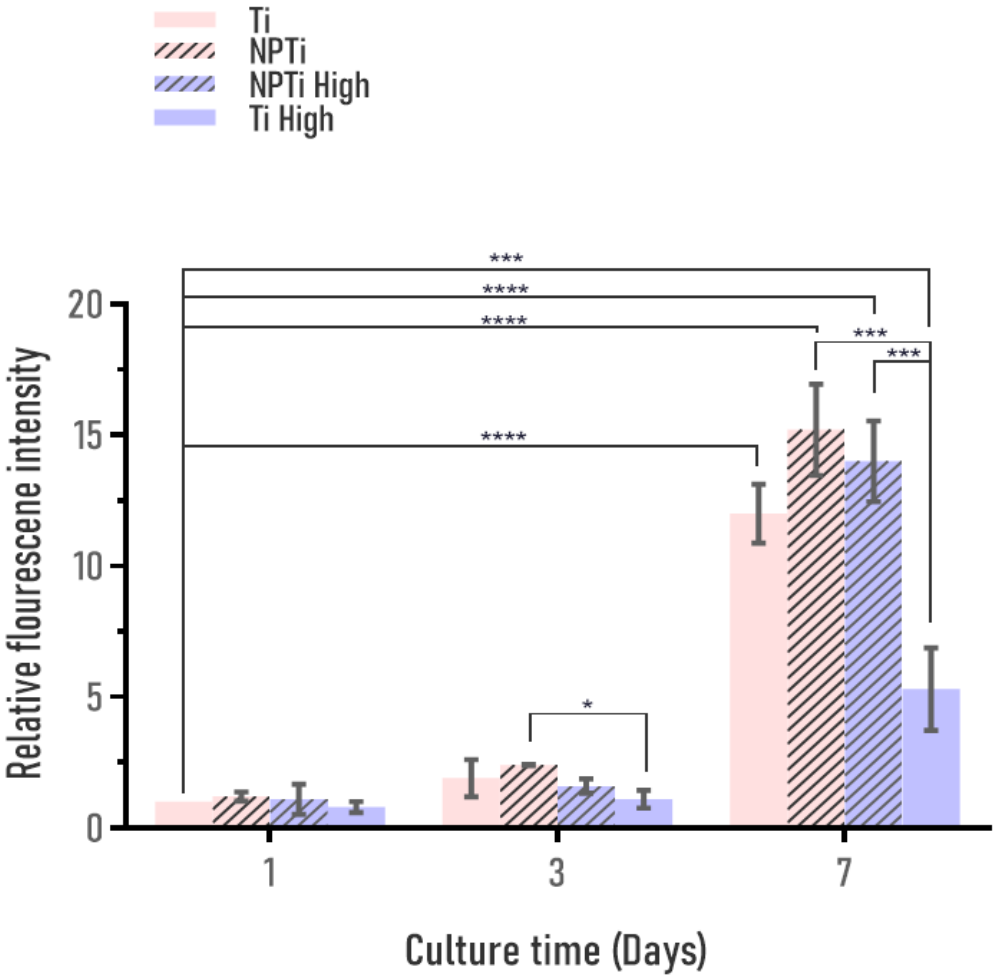

Figure 4.8: MG-63 cell proliferation analysis by PrestoBlue assay

Fluorescence intensity on Days 1, 3 and 7. (ANOVA test, (n=4): * = $p < 0.05$, ** = $p < 0.01$, ***$p < 0.0005$, ****$p < <0.0001$).

To further investigate the effects of nanoporous titanium on cell proliferation in normal and hyperglycemic conditions, PrestoBlue analysis was carried out. **Figure 4.8** displays the PrestoBlue analysis of cell proliferation showing a considerable difference between MG-63 cell proliferation at days 1, 3 and 7; that was determined by analyzing data collected from a total number of 160 samples during 4 independent experiments with 20 samples in each experimental condition and timepoint (n=4). Cell proliferation quantified at days 1 and 3 by PrestoBlue assay confirmed results obtained by the Ki-67 analysis. Variation in cell proliferation was not observed in relation to the substrate at day 1, a higher non-significant proliferation was observed on Ti and NPTi substrates in normal glucose condition samples in comparison to the hyperglycemic state. Cells in normal glucose levels continued to show a similar trend to earlier days at day 7; however, significant differences were observed in high glucose conditions. In particular, cell proliferation on NPTi samples showed a 3-fold increase compared to Ti samples in hyperglycemic conditions. Furthermore, NPTi samples in hyperglycemic conditions showed almost similar cell proliferation to samples in normal glucose conditions. This reinforces the concept that direct topographical cueing may be able to rescue MG63 cells from the negative effects of hyperglycemia.

Osteoblast proliferation is an essential aspect that affects the osseointegration of implants. In this study, both Ki-67 analysis and PrestoBlue assay at days 3 and 7 revealed that high glucose suppresses the proliferation of osteoblasts, thereby confirming the widely accepted theory based on previously published experimental evidence of such detrimental effects [70], [99].

However, my results reveal that the direct physicochemical cueing exerted by nanoporous surfaces is independent of glucose levels and could compensate for the detrimental effects of hyperglycemia in MG-63 cells.

4.2.3 Differentiation Analysis

In addition to cell adhesion and proliferation, surface nanotopography also affects the differentiation of cells[70], [107], [128]. In this context, I investigated the osteoinductive capabilities of nanoporous titanium by assessing the osteoblasts differentiation markers, RUNX2, OCN and ALP in normal and high glucose conditions by analyzing the data collected from a total number of 160 samples during 4 independent experiments with 20 samples in each experimental condition (n=4) at day 7. Furthermore, long terms effects of ALP activity were also examined at days 7, 14 and 21.

RUNX2 is an essential transcription factor called the master regulator, as it is the initial gene for several genetic expression pathways, especially in the early stages of differentiation[101]. A qualitative assessment was initially performed using images obtained from immunofluorescence staining (**Figure 4.9**). **Figure 4.11** shows the representative graph of the significant differences in RUNX2 expression between nanoporous and untreated titanium under experimental conditions at day 7, obtained from the quantitative assessment of results obtained after western blotting. I detected a significant increase in RUNX2 expression in cells on NTPi samples compared to Ti samples in normal glucose conditions, which is indicative of the fact that oxidative nanopatterning treatment elicits osteogenic induction. The trend found here corresponds to that of previous studies that have shown that topographical modification of titanium is effective in lineage guidance[9], [70], [99].

Furthermore, a significant increase in expression was also observed in NPTi samples under hyperglycemic conditions compared to Ti samples under the same conditions. Even though the increase was not on par with that observed in normal glucose levels, which was expected as hyperglycemia has shown to have detrimental effects on RUNX2 expression levels[107], it is still a remarkable result as it highlights the ability of oxidative nanopatterning to attenuate the effects of hyperglycemia on osteogenic expression.

To further the investigation on osteogenic differentiation, the expression of OCN was also quantified following a qualitative assessment (**Figure 4.10**). OCN is a protein secreted by osteoblasts, identified as a late differentiation marker and a hormone responsible for maintaining glucose homeostasis [108], [129]. The protein quantification (**Figure 4.12**) obtained from western blotting showed a significantly enhanced level from cells cultured on NPTi samples compared to Ti in normal glucose levels. This further reinforces the previous knowledge that nanoporous titanium stimulates late osteogenic differentiation. One interesting aspect that emerged from the analysis is that NPTi samples in high glucose showed almost similar expression to that observed on NPTi samples in normal glucose conditions, along with a significant increase compared to Ti-high glucose samples. The higher expression observed in cells on nanoporous samples, regardless of experimental condition, is noteworthy since OCN has been shown to have an association with glucose homeostasis[129]. Therefore, although farfetched based on these preliminary data, it could be nonetheless extrapolated that the higher expression of OCN by MG-63 cells on nanoporous titanium would thereby have dual effects in *in-vivo* hyperglycemic conditions. In particular, it would not only attenuate the negative

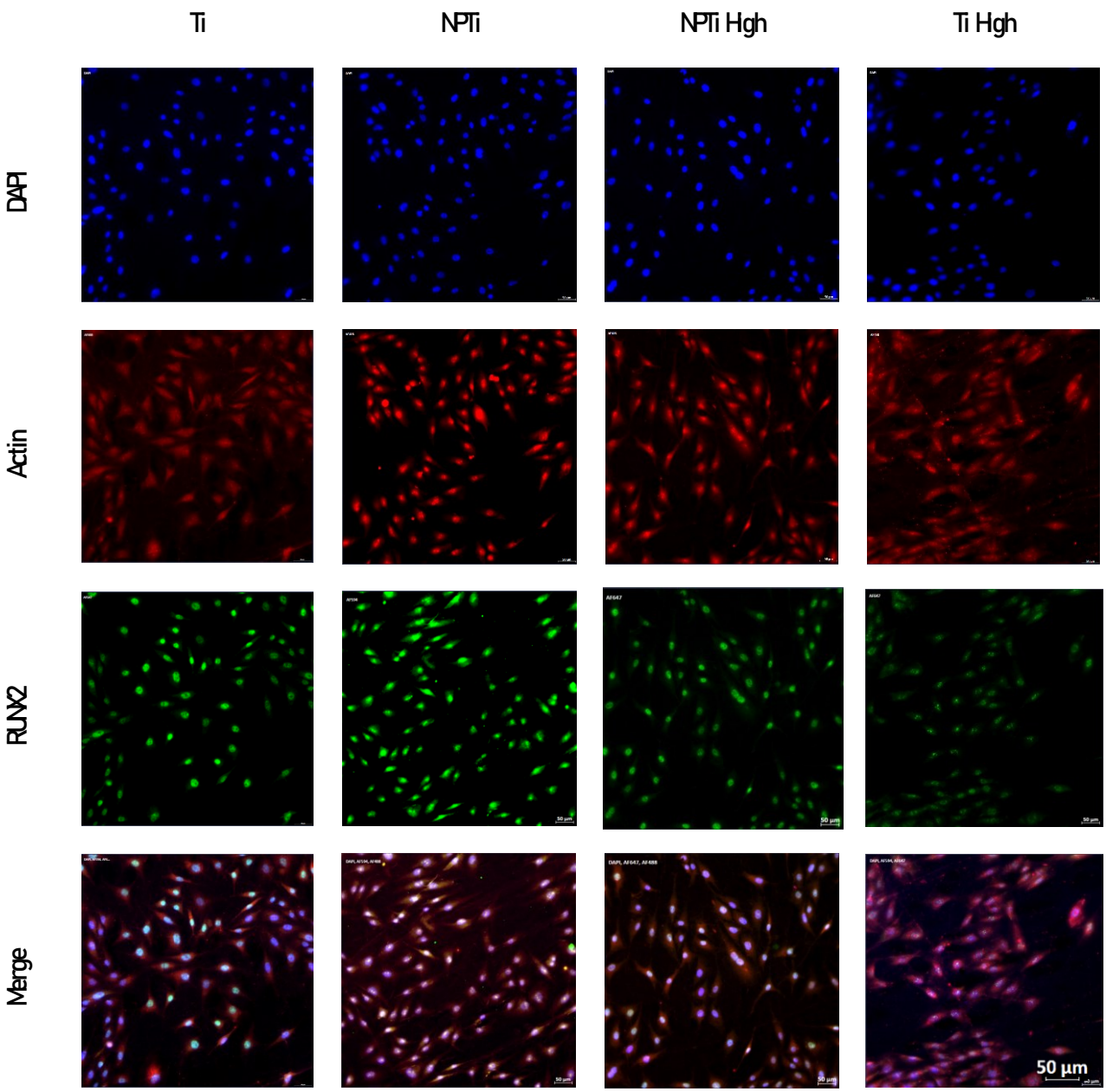

Figure 4.9: Immunofluorescence images of RUNX2 expression at day 7

Representative images of immunofluorescence staining, blue (DAPI), red (Actin), RUNX2 (green), *Scale bar=50µm;* Ti: Control titanium in normal glucose conditions, NPTi: Nanoporous titanium in normal glucose conditions, Ti High: Control titanium in high glucose conditions, NPTi High: Nanoporous titanium in high glucose conditions.

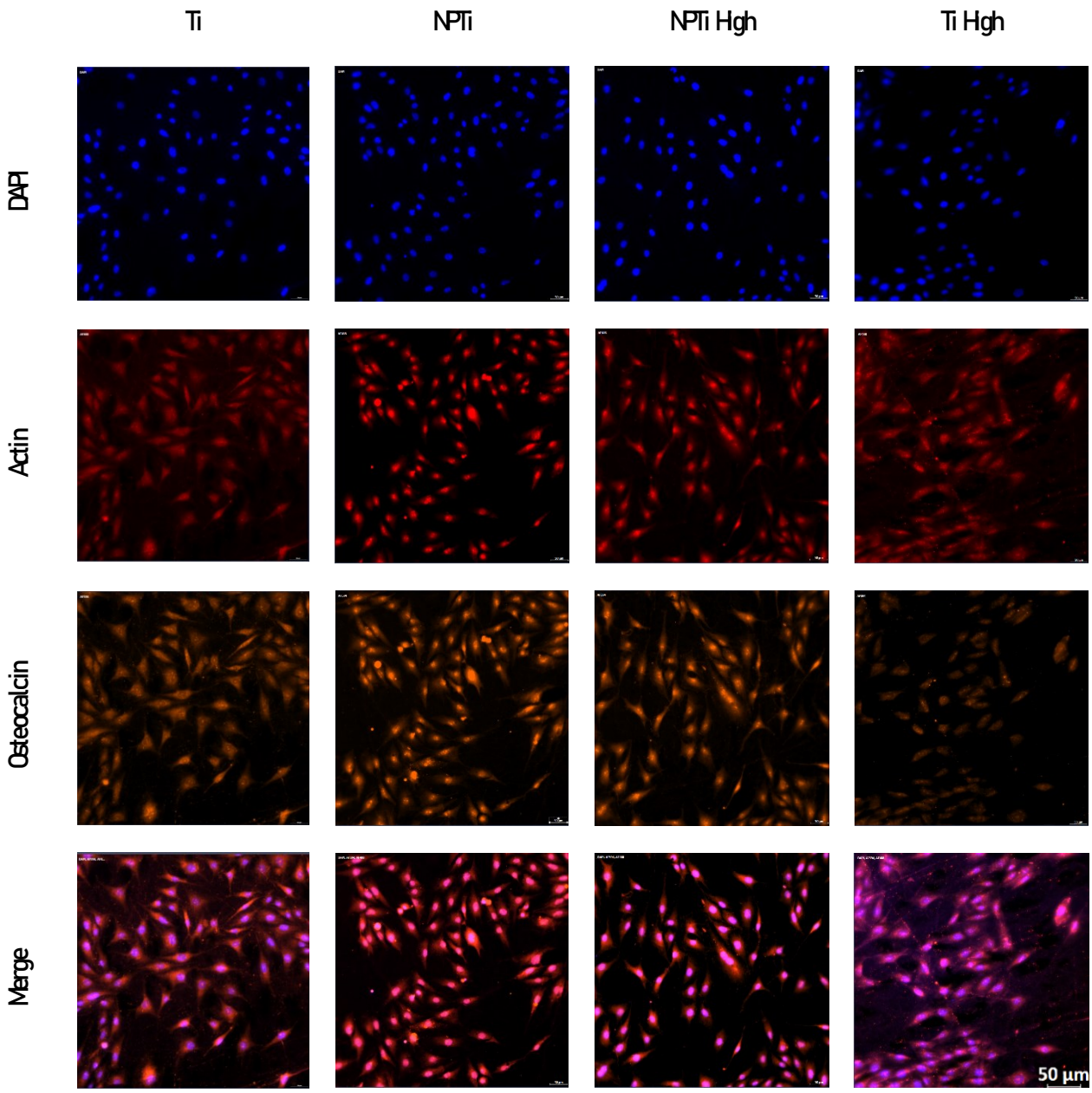

Figure 4.10: Immunofluorescence images of OCN expression at day 7

Representative images of immunofluorescence staining, blue (DAPI), red (Actin), OCN (orange), *Scale bar=50µm;* Ti: Control titanium in normal glucose conditions, NPTi: Nanoporous titanium in normal glucose conditions, Ti High: Control titanium in high glucose conditions, NPTi High: Nanoporous titanium in high glucose conditions

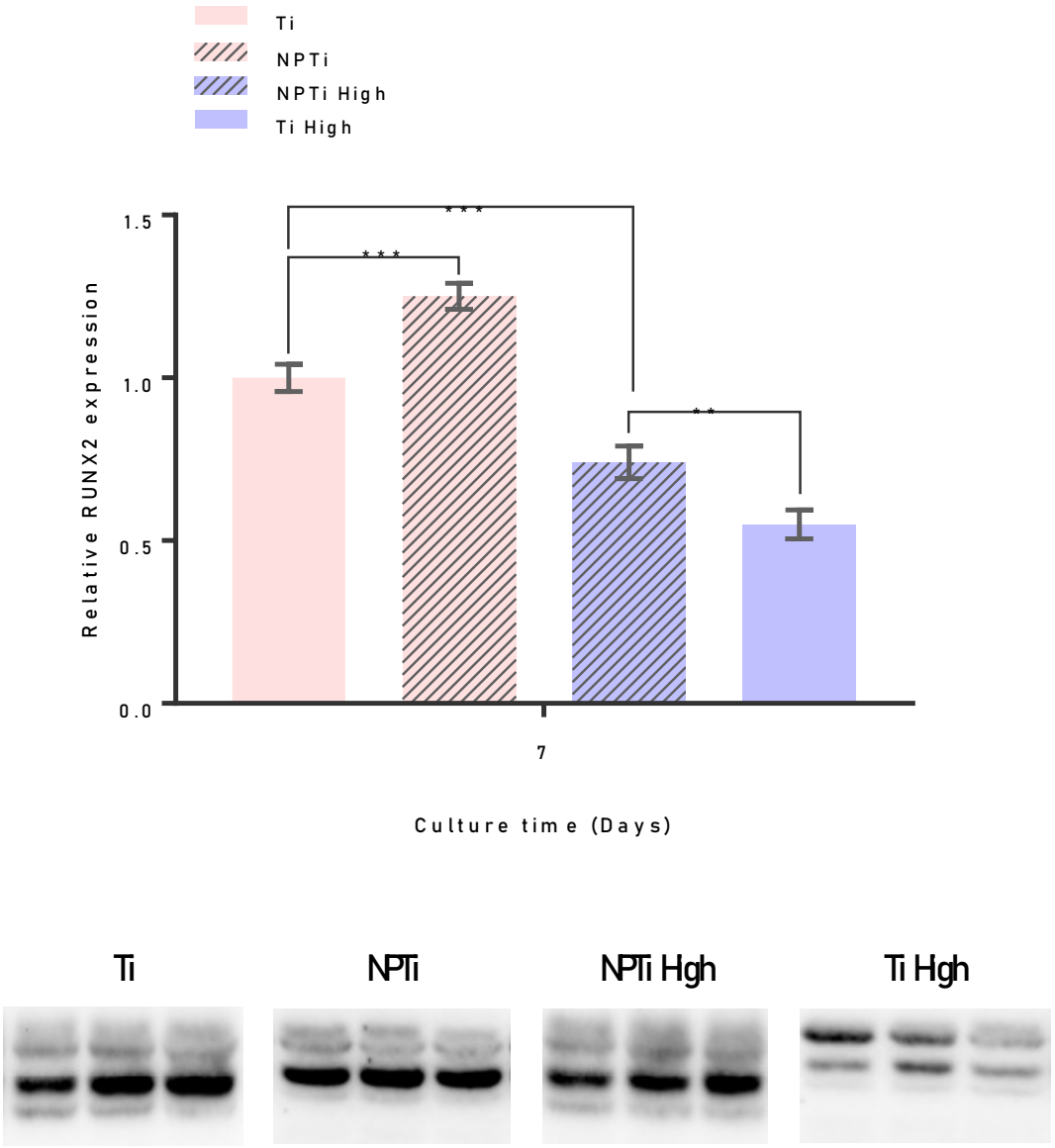

Figure 4.11: RUNX2 Differentiation in MG-63 cells

Western blot analysis for RUNX2 (ANOVA test, (n=4): ** = p < 0.01, ***p< 0.0005, ****p< <0.0001). The western blot images are representative.

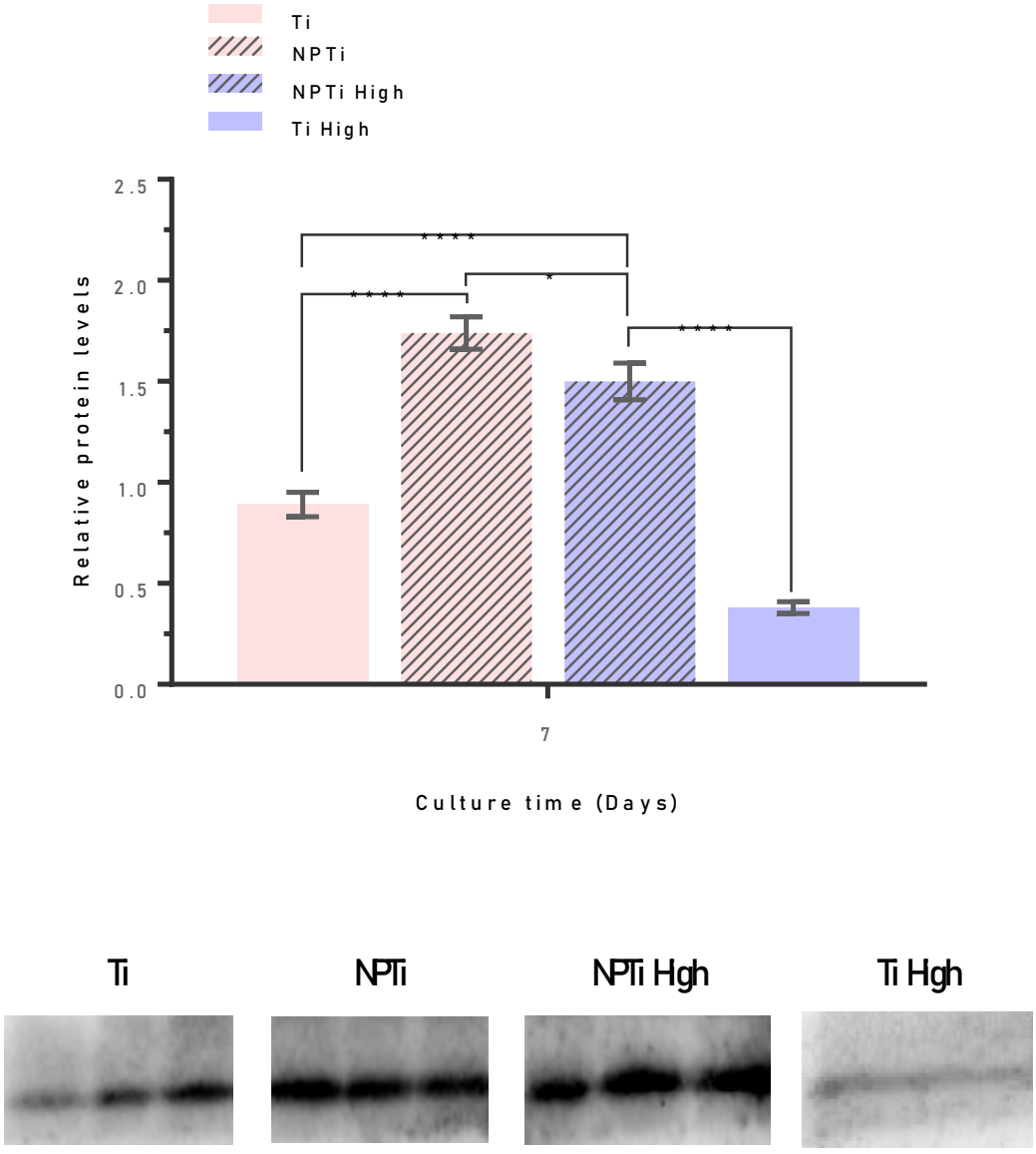

Figure 4.12: Osteocalcin Differentiation in MG-63 cells

Western blot analysis for Osteocalcin. (ANOVA test, (n=4): * = $p < 0.05$, **** = $p < 0.0001$). The western blot images are representative.

effect of hyperglycemia on osteogenic differentiation, but it would also lead to better insulin signalling, ultimately helping with glucose level maintenance. In fact, OCN has been identified as a hormone secreted by osteoblasts responsible for insulin expression through a regulatory loop monitored by insulin receptors present on osteoblasts. Overall concluding that OCN is essential in maintaining glucose homeostasis and insulin signalling.[111]

In this context, ALP is another critical marker recognized widely for osteogenic differentiation. Therefore, ALP activity was used as an indicator of osteoblast maturation and differentiation (**Figure 4.13**). My findings show that cells in normal glucose showed similar activity at day 7 regardless of the substrate, which was followed by a rise in activity in cells on NPTi samples at day 14, although the rise was not statistically significant. Day 21 marked a decline in ALP activity in cells on NPTi, although Ti samples showed similar results as day 14. Similar trends in ALP activity under normal conditions have been previously reported by De Oliveira *et al.* in an *in-vitro* study [26], although the mechanisms responsible for these observations are undetermined.

However, observations in higher glucose conditions were contradictory to those seen in normal glucose conditions. Even though day 7 acted as an exception and reported a lower ALP activity in cells in high glucose conditions compared to normal glucose conditions, a significantly elevated ALP activity in cells was recorded henceforth at day 14 and day 21 in high glucose conditions as opposed to normal conditions. In terms of experimental samples, cells on NPTi samples showed significantly increased results than Ti samples in high glucose conditions at all time points, highlighting the ability of oxidative nanopatterning to attenuate the effects of hyperglycemia on osteogenic expression (**Figure 4.13**).

ALP activity was monitored for longer intervals (Day 7 to day 21), as opposed to the other differentiation markers, which were only monitored for 7 days as I wanted to investigate its expression in high glucose conditions during extended periods, as differences in literature have been observed in this regard.

My results in high glucose conditions contradicted those obtained by Jiang *et al.* [70], who observed a lower ALP activity in high glucose conditions during extended periods. However, they were in agreement with those obtained by Botolin *et al.* [107], who also reported a high ALP activity in osteoblasts in high glucose conditions during extended periods.

These contradictory results may be due to the differences in incubation times. The Pre-conditioning step in my work increases the incubation time experienced by osteoblasts, and

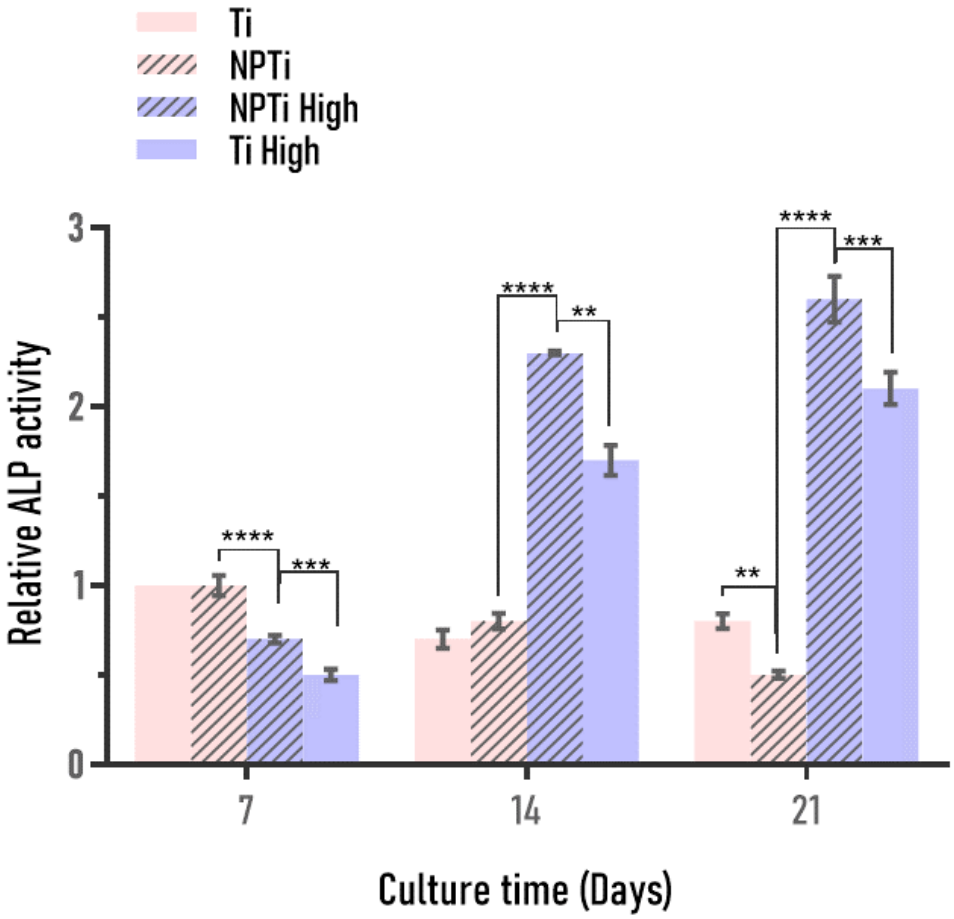

Figure 4.13: ALP activity of MG-63 cells

The relative ALP activity of MG-63 cells measured on Day 7, 14 and 21. (ANOVA test, (n=4): * = $p < 0.05$, ** = $p < 0.01$, ***$p < 0.0005$, ****$p < <0.0001$)

this could be compared to the chronic conditions described by Botolin et al.[107], characterized by higher ALP levels in osteoblasts. Chronic conditions negate the effect of hyperosmotic stress (a condition observed in hyperglycemia which leads to cell shrinking), which causes an effect on osteoblasts marker gene expression[107]. This could thus be the reason for the changes observed. However, additional studies to support these findings are required.

Effective osteoblasts adhesion, proliferation and differentiation are amongst the important biological events required for the effective bone tissue integration of implants. In this regard, nanoporous titanium has been shown to improve osteoblast bone-forming functionalities when compared to the untreated metal[9], [27], [28], [37]. However, whether these properties can rescue cells under hyperglycemic conditions was never investigated. The development and investigation of novel nanostructured surfaces capable of rescuing cells from challenging conditions would cast new light on the mechanisms underlying cell-surface interactions and therefore unlock the key to better-performing biomaterials. To this end, this study focused on characterizing osteoblast bone-forming capabilities of NPTis under the detrimental growing environment in hyperglycemia known to affect proliferation and differentiation.
As a result of my findings, nanoporous titanium has been demonstrated to compensate for some of the detrimental effects, thereby opening the door for future studies aimed at better understanding the interplay between hyperglycemia, reduced proliferation and differentiation, and countereffects exerted by the nanostructured surface.

Chapter 5

CONCLUSIONS AND FUTURE DIRECTIONS

This study provides insights into the use of nanoscale surface modifications to develop biocompatible metals with enhanced surfaces that are able to counter challenging conditions like hyperglycemia. To this effect, we investigated whether the use of oxidative nanopatterning, a technique previously proven to increase the bioactivity of titanium, is capable of ameliorating the effects of high glucose content on osteoblasts functionality. To this end, I was able to demonstrate that nanoporous surface resulting from oxidative nanopatterning provides bioactive effects that extend to both normal and high glucose levels. An increased cell spreading, along with more rapid proliferation and upregulation in differentiation, was observed in osteoblasts on nanoporous titanium, even in hyperglycemic conditions. These results demonstrate the capabilities of the treatment in rescuing osteoblastic cells as these cellular activities are known to be severally reduced due to hyperglycemic conditions. Moving forward, a more sophisticated understanding of the underlying mechanisms responsible for the beneficial role of nanostructured titanium surfaces will provide deeper insights into cell-substrate interactions. Ultimately, this new knowledge is expected to support the development of novel orthopedic and dental implantable biomaterials that are capable of exerting positive effects on cells, even if these are in sub-optimal conditions.

I hope that this study's findings will ultimately provide the foundation for future work aimed at understanding the role of nanoscale surface modifications in the development of next-generation functional biomaterials.

Chapter 6

BIBLIOGRAPHY

[1] B. Ganesan and W. T. J., "Nanotechnology and biomaterials for orthopedic medical applications," *Nanomedicine*, vol. 1, no. 2, pp. 169–176, 2006.

[2] C. J. Bettinger, R. Langer, and J. T. Borenstein, "'Engineering Substrate Micro-and Nanotopography to Control Cell Function' Lead-In," doi: 10.1002/anie.200805179.

[3] E. K. F. Yim and K. W. Leong, "Significance of synthetic nanostructures in dictating cellular response," *Nanomedicine Nanotechnology, Biol. Med.*, vol. 1, no. 1, pp. 10–21, Mar. 2005, doi: 10.1016/J.NANO.2004.11.008.

[4] L. Richert *et al.*, "Surface nanopatterning to control cell growth," *Adv. Mater.*, vol. 20, no. 8, pp. 1488–1492, 2008, doi: 10.1002/adma.200701428.

[5] A. Marzban, P. Ranjbarvan, and A. Golchin, "Cell-Surface Interaction and Biological Behavior of Cells: An Overview," *Regen. Reconstr. Restor.*, vol. 4, no. 4, pp. 121–129, 2019, doi: 10.22037/rrr.v4i4.29799.

[6] M. Gajiwala *et al.*, "Influence of surface modification of titanium implants on improving osseointegration: An in vitro study," *J. Prosthet. Dent.*, vol. 126, no. 3, pp. 405.e1-405.e7, 2021, doi: 10.1016/j.prosdent.2021.06.034.

[7] E. P. Su *et al.*, "Effects of titanium nanotubes on the osseointegration, cell differentiation, mineralisation and antibacterial properties of orthopaedic implant surfaces," *Bone Jt. J.*, vol. 100B, no. 1, pp. 9–16, 2018, doi: 10.1302/0301-620X.100B1.BJJ-2017-0551.R1.

[8] W. Meng, Y. Zhou, Y. Zhang, Q. Cai, L. Yang, and B. Wang, "Effects of hierarchical micro/nano-textured titanium surface features on osteoblast-specific gene expression," *Implant Dent.*, vol. 22, no. 6, pp. 656–661, 2013, doi: 10.1097/01.id.0000434273.22605.78.

[9] P. Tambasco De Oliveira and A. Nanci, "Nanotexturing of titanium-based surfaces upregulates expression of bone sialoprotein and osteopontin by cultured osteogenic cells," *Biomaterials*, vol. 25, no. 3, pp. 403–413, 2004, doi: 10.1016/S0142-9612(03)00539-8.

[10] R. Van Noort, “Titanium: The implant material of today,” *J. Mater. Sci.*, vol. 22, no. 11, pp. 3801–3811, Nov. 1987, doi: 10.1007/BF01133326/METRICS.

[11] M. Kaur and K. Singh, “Review on titanium and titanium based alloys as biomaterials for orthopaedic applications,” *Mater. Sci. Eng. C*, vol. 102, pp. 844–862, Sep. 2019, doi: 10.1016/J.MSEC.2019.04.064.

[12] A. J. Steeves *et al.*, “The implication of spatial statistics in human mesenchymal stem cell response to nanotubular architectures,” *Int. J. Nanomedicine*, 2020, doi: 10.2147/IJN.S238280.

[13] I. Lauria, T. N. Kutz, F. Böke, S. Rütten, D. Zander, and H. Fischer, “Influence of nanoporous titanium niobium alloy surfaces produced via hydrogen peroxide oxidative etching on the osteogenic differentiation of human mesenchymal stromal cells,” *Mater. Sci. Eng. C*, vol. 98, no. December 2018, pp. 635–648, 2019, doi: 10.1016/j.msec.2019.01.023.

[14] R. de B. e. L. Bueno, P. Adachi, L. M. S. de Castro-Raucci, A. L. Rosa, A. Nanci, and P. T. de Oliveira, “Oxidative nanopatterning of titanium surfaces promotes production and extracellular accumulation of osteopontin,” *Braz. Dent. J.*, vol. 22, no. 3, pp. 179–184, 2011, doi: 10.1590/s0103-64402011000300001.

[15] F. Vetrone *et al.*, “Nanoscale oxidative patterning of metallic surfaces to modulate cell activity and fate,” *Nano Lett.*, vol. 9, no. 2, pp. 659–665, 2009, doi: 10.1021/n1803051f.

[16] Z. Zhao, J. Tian, Y. Sang, A. Cabot, and H. Liu, “Structure, synthesis, and applications of TiO2 nanobelts,” *Adv. Mater.*, vol. 27, no. 16, pp. 2557–2582, 2015, doi: 10.1002/adma.201405589.

[17] Y. Hou *et al.*, “Effects of titanium nanoparticles on adhesion, migration, proliferation, and differentiation of mesenchymal stem cells,” *Int. J. Nanomedicine*, vol. 8, pp. 3619–3630, Sep. 2013, doi: 10.2147/IJN.S38992.

[18] K. S. Brammer, S. Oh, J. O. Gallagher, and S. Jin, “Enhanced cellular mobility guided by TiO2 nanotube surfaces,” *Nano Lett.*, 2008, doi: 10.1021/nl072572o.

[19] D. Wang, G. He, Y. Tian, N. Ren, W. Liu, and X. Zhang, “Dual effects of acid etching on cell responses and mechanical properties of porous titanium with controllable open-porous structure,” *J. Biomed. Mater. Res. B. Appl. Biomater.*, vol. 108, no. 6, pp. 2386–2395, Aug. 2020, doi: 10.1002/JBM.B.34571.

[20] S. Minagar, J. Wang, C. C. Berndt, E. P. Ivanova, and C. Wen, “Cell response of anodized nanotubes on titanium and titanium alloys,” *Journal of Biomedical Materials Research - Part A*. 2013, doi: 10.1002/jbm.a.34575.

[21] M. F. Sola-Ruiz, C. Perez-Martinez, C. Labaig-Rueda, C. Carda, and J. J. Martín De Llano, "Behavior of human osteoblast cells cultured on titanium discs in relation to surface roughness and presence of melatonin," *Int. J. Mol. Sci.*, vol. 18, no. 4, 2017, doi: 10.3390/ijms18040823.

[22] L. Tan *et al.*, "Engineered probiotics biofilm enhances osseointegration via immunoregulation and anti-infection," *Sci. Adv*, vol. 6, pp. 5723–5736, 2020, Accessed: Dec. 27, 2022. [Online]. Available: https://www.science.org.

[23] C. Hou *et al.*, "Surface Modification Techniques to Produce Micro/Nano-scale Topographies on Ti-Based Implant Surfaces for Improved Osseointegration," *Front. Bioeng. Biotechnol.*, vol. 10, no. March, pp. 1–16, 2022, doi: 10.3389/fbioe.2022.835008.

[24] L. Richert, F. Variola, F. Rosei, J. D. Wuest, and A. Nanci, "Adsorption of proteins on nanoporous Ti surfaces," *Surf. Sci.*, vol. 604, no. 17–18, pp. 1445–1451, Aug. 2010, doi: 10.1016/J.SUSC.2010.05.007.

[25] F. Variola, J. H. Yi, L. Richert, J. D. Wuest, F. Rosei, and A. Nanci, "Tailoring the surface properties of Ti6Al4V by controlled chemical oxidation," *Biomaterials*, vol. 29, no. 10, pp. 1285–1298, Apr. 2008, doi: 10.1016/J.BIOMATERIALS.2007.11.040.

[26] P. T. De Oliveira, S. F. Zalzal, M. M. Beloti, A. L. Rosa, and A. Nanci, "Enhancement of in vitro osteogenesis on titanium by chemically produced nanotopography," *J. Biomed. Mater. Res. Part A*, vol. 80A, no. 3, pp. 554–564, Mar. 2007, doi: 10.1002/JBM.A.30955.

[27] F. Vetrone *et al.*, "Nanoscale Oxidative Patterning of Metallic Surfaces to Modulate Cell Activity and Fate," *Nano Lett.*, vol. 9, no. 2, pp. 659–665, Feb. 2009, doi: 10.1021/NL803051F.

[28] A. Ketabchi, A. Weck, and F. Variola, "Influence of oxidative nanopatterning and anodization on the fatigue resistance of commercially pure titanium and Ti–6Al–4V," *J. Biomed. Mater. Res. Part B Appl. Biomater.*, vol. 103, no. 3, pp. 563–571, Apr. 2015, doi: 10.1002/JBM.B.33227.

[29] G. Tan *et al.*, "Controlled oxidative nanopatterning of microrough titanium surfaces for improving osteogenic activity," *J. Mater. Sci. Mater. Med.*, vol. 25, no. 8, pp. 1875–1884, 2014, doi: 10.1007/s10856-014-5232-2.

[30] A. Mellado Valero, J. C. Ferrer García, A. Herrera Ballester, and C. Labaig Rueda, "Effects of diabetes on the osseointegration of dental implants," *Med. Oral Patol. Oral Cir. Bucal*, vol. 12, no. 1, pp. 26–31, 2007.

[31] P. Farzad, L. Andersson, and J. Nyberg, “Dental Implant Treatment in Diabetic Patients,” *Implant Dent.*, vol. 11, no. 3, pp. 262–267, 2002, doi: 10.1097/00008505-200207000-00011.

[32] “Diabetes rates continue to climb in Canada - Diabetes Canada.” https://www.diabetes.ca/media-room/press-releases/diabetes-rates-continue-to-climb-in-canada (accessed Dec. 24, 2022).

[33] J. W. Yoon and H. S. Jun, “Autoimmune destruction of pancreatic beta cells,” *Am. J. Ther.*, vol. 12, no. 6, pp. 580–591, Nov. 2005, doi: 10.1097/01.MJT.0000178767.67857.63.

[34] G. L. King, “The role of inflammatory cytokines in diabetes and its complications,” *J. Periodontol.*, vol. 79, no. 8 Suppl, pp. 1527–1534, Aug. 2008, doi: 10.1902/JOP.2008.080246.

[35] “What is Diabetes? | NIDDK.” https://www.niddk.nih.gov/health-information/diabetes/overview/what-is-diabetes (accessed Dec. 03, 2022).

[36] I. Yamawaki, Y. Taguchi, S. Komasa, A. Tanaka, and M. Umeda, “Effects of glucose concentration on osteogenic differentiation of type II diabetes mellitus rat bone marrow-derived mesenchymal stromal cells on a nano-scale modified titanium,” *J. Periodontal Res.*, vol. 52, no. 4, pp. 761–771, 2017, doi: 10.1111/jre.12446.

[37] J. H. Yi *et al.*, “Characterization of a bioactive nanotextured surface created by controlled chemical oxidation of titanium,” *Surf. Sci.*, vol. 600, no. 19, pp. 4613–4621, 2006, doi: 10.1016/j.susc.2006.07.053.

[38] A. Bashan, R. P. Bartsch, J. W. Kantelhardt, shlomo Havlin, and P. Ch Ivanov, “network physiology reveals relations between network topology and physiological function,” *Nat. Commun.*, 2012, doi: 10.1038/ncomms1705.

[39] R. P. Bartsch, K. K. L Liu, A. Bashan, and P. Ch Ivanov, “Network Physiology: How Organ Systems Dynamically Interact,” 2015, doi: 10.1371/journal.pone.0142143.

[40] C. A. Custódio and J. F. Mano, “Europe PMC Funders Group Cell surface engineering to control cellular interactions,” vol. 2, no. 5, pp. 376–384, 2019, doi: 10.1002/cnma.201600047.Cell.

[41] F. Villanueva-Flores, A. Castro-Lugo, O. T. Ramírez, and L. A. Palomares, “Understanding cellular interactions with nanomaterials: towards a rational design of medical nanodevices,” *Nanotechnology*, vol. 31, no. 13, Mar. 2020, doi: 10.1088/1361-6528/AB5BC8.

[42] G. Zhou, B. Zhang, G. Tang, X. F. Yu, and M. Galluzzi, “Cells nanomechanics by

atomic force microscopy: focus on interactions at nanoscale," *https://doi.org/10.1080/23746149.2020.1866668*, vol. 6, no. 1, p. 1866668, 2021, doi: 10.1080/23746149.2020.1866668.

[43] A. S. G. Curtis *et al.*, "Cell interactions at the nanoscale: Piezoelectric stimulation," *IEEE Trans. Nanobioscience*, vol. 12, no. 3, pp. 247–254, 2013, doi: 10.1109/TNB.2013.2257837.

[44] S. Xia and P. Kanchanawong, "Nanoscale mechanobiology of cell adhesions," *Semin. Cell Dev. Biol.*, vol. 71, pp. 53–67, Nov. 2017, doi: 10.1016/J.SEMCDB.2017.07.029.

[45] R. Staruch, M. Griffin, and P. Butler, "Nanoscale Surface Modifications of Orthopaedic Implants: State of the Art and Perspectives," *Open Orthop. J.*, vol. 10, no. 1, pp. 920–938, Jan. 2017, doi: 10.2174/1874325001610010920.

[46] F. Variola, J. B. Brunski, G. Orsini, P. Tambasco De Oliveira, R. Wazen, and A. Nanci, "Nanoscale surface modifications of medically-relevant metals: state-of-the art and perspectives," *Nanoscale*, vol. 3, no. 2, p. 335, Feb. 2011, doi: 10.1039/C0NR00485E.

[47] N. C. Verissimo, S. Chung, and T. J. Webster, "New nanoscale surface modifications of metallic biomaterials," *Surf. Coat. Modif. Met. Biomater.*, pp. 249–273, Jan. 2015, doi: 10.1016/B978-1-78242-303-4.00008-9.

[48] D. S. Nakonieczny, M. Antonowicz, and Z. Paszenda, "Surface modification methods of ceramic filler in ceramic-carbon fibre composites for bioengineering applications - A systematic review," *Rev. Adv. Mater. Sci.*, vol. 59, no. 1, pp. 586–609, Jan. 2020, doi: 10.1515/RAMS-2020-0024/XML.

[49] S. K. Nemani *et al.*, "Surface Modification of Polymers: Methods and Applications," *Adv. Mater. Interfaces*, vol. 5, no. 24, p. 1801247, Dec. 2018, doi: 10.1002/ADMI.201801247.

[50] L. Xie *et al.*, "Surface Modification Techniques of Titanium and its Alloys to Functionally Optimize Their Biomedical Properties: Thematic Review," 2020, doi: 10.3389/fbioe.2020.603072.

[51] Y. Zhukova and E. V. Skorb, "Cell Guidance on Nanostructured Metal Based Surfaces," *Adv. Healthc. Mater.*, vol. 6, no. 7, 2017, doi: 10.1002/adhm.201600914.

[52] W. Jin and P. K. Chu, "Orthopedic implants," *Encycl. Biomed. Eng.*, vol. 1–3, pp. 425–439, Jan. 2019, doi: 10.1016/B978-0-12-801238-3.10999-7.

[53] G. W. Hastings, "Biomedical engineering and materials for orthopaedic implants," *J. Phys. E.*, vol. 13, no. 6, p. 599, Jun. 1980, doi: 10.1088/0022-3735/13/6/001.

[54] T. Kim, C. W. See, X. Li, and D. Zhu, "Orthopedic implants and devices for bone

fractures and defects: Past, present and perspective," *Eng. Regen.*, vol. 1, no. June, pp. 6–18, 2020, doi: 10.1016/j.engreg.2020.05.003.

[55] "Sci-Hub | A systematic review of the influence of different titanium surfaces on proliferation, differentiation and protein synthesis of osteoblast-like MG63 cells. Clinical Oral Implants Research, 15(6), 683–692 | 10.1111/j.1600-0501.2004.01054.x." https://sci-hub.se/10.1111/j.1600-0501.2004.01054.x (accessed Oct. 18, 2022).

[56] K. C. Popat, L. Leoni, C. A. Grimes, and T. A. Desai, "Influence of engineered titania nanotubular surfaces on bone cells," *Biomaterials*, vol. 28, no. 21, pp. 3188–3197, Jul. 2007, doi: 10.1016/J.BIOMATERIALS.2007.03.020.

[57] H. Li *et al.*, "Nanoscale Modification of Titanium Implants Improves Behaviors of Bone Mesenchymal Stem Cells and Osteogenesis In Vivo," *Oxid. Med. Cell. Longev.*, vol. 2022, 2022, doi: 10.1155/2022/2235335.

[58] D. C. Momete and D. S. Vasilescu, "Synthetic materials used in orthopedy," *Rev. Roum. Chim.*, vol. 49, no. 12, pp. 955–964, 2004.

[59] M. Navarro, A. Michiardi, O. Castaño, and J. A. Planell, "Biomaterials in orthopaedics," *Journal of the Royal Society Interface*, vol. 5, no. 27. 2008, doi: 10.1098/rsif.2008.0151.

[60] B. Ratner, A. Hoffman, F. Schoen, and J. Lemons, *Biomaterials science: an introduction to materials in medicine*. 2004.

[61] "Macromolecular Bioscience - 2022 - Alvarez Echaz - Recent Advances in Synthetic and Natural Biomaterials-Based Therapy for.pdf." .

[62] Y. Li, C. Wong, J. Xiong, P. Hodgson, and C. Wen, "Cytotoxicity of titanium and titanium alloying elements," *J. Dent. Res.*, vol. 89, no. 5, pp. 493–497, 2010, doi: 10.1177/0022034510363675.

[63] M. L. Vera, E. Linardi, L. Lanzani, C. Mendez, C. E. Schvezov, and A. E. Ares, "Corrosion resistance of titanium dioxide anodic coatings on Ti–6Al–4V," *Mater. Corros.*, vol. 66, no. 10, pp. 1140–1149, Oct. 2015, doi: 10.1002/MACO.201407988.

[64] X. Yan and X. Chen, "Titanium Dioxide Nanomaterials," 2011, doi: 10.1002/9781119951438.eibc2335.

[65] foreword. DAVIES, J.E., ed. VACANTI, J.P., *Bone Engineering. First Edition.* .

[66] F. Varíola *et al.*, "Improving biocompatibility of implantable metals by nanoscale modification of surfaces: An overview of strategies, fabrication methods, and challenges," *Small*, vol. 5, no. 9, pp. 996–1006, 2009, doi: 10.1002/smll.200801186.

[67] C. Ohtsuki, M. Kamitakahara, and T. Miyazaki, "Bioactive ceramic-based materials with designed reactivity for bone tissue regeneration," doi:

10.1098/rsif.2008.0419.focus.

[68] J. Strnad, Z. Strnad, and J. Šesták, "Physico-chemical properties and healing capacity of potentially bioactive titanium surface," *J. Therm. Anal. Calorim.*, vol. 88, no. 3, pp. 775–779, 2007, doi: 10.1007/s10973-006-8295-6.

[69] K. Y. Hung, Y. C. Lin, and H. P. Feng, "The Effects of Acid Etching on the Nanomorphological Surface Characteristics and Activation Energy of Titanium Medical Materials," *Mater. (Basel, Switzerland)*, vol. 10, no. 10, Oct. 2017, doi: 10.3390/MA10101164.

[70] H. Jiang *et al.*, "The Effects of Hierarchical Micro/Nano-Structured Titanium Surface on Osteoblast Proliferation and Differentiation under Diabetic Conditions," *Implant Dent.*, vol. 26, no. 2, pp. 263–269, 2017, doi: 10.1097/ID.0000000000000576.

[71] M. Gruening, S. Neuber, K. Fricke, C. A. Helm, and B. Nebe, "Cell-Material Interaction-Spreading Course correlates with Surface Charge," no. 1, pp. 2020–2029, doi: 10.34297/AJBSR.2020.09.001341.

[72] T. Hanawa, "In vivo metallic biomaterials and surface modification," *Mater. Sci. Eng. A*, vol. 267, no. 2, pp. 260–266, Jul. 1999, doi: 10.1016/S0921-5093(99)00101-X.

[73] M. Li, M. J. Mondrinos, X. Chen, M. R. Gandhi, F. K. Ko, and P. I. Lelkes, "The influence of the crystallinity of electrostatic spray deposition-derived coatings on osteoblast-like cell behavior, in vitro," *J. Biomed. Mater. Res. Part A*, vol. 79, no. 4, pp. 963–73, 2006, doi: 10.1002/jbm.a.

[74] C. Massaro, M. A. Baker, F. Cosentino, P. A. Ramires, S. Klose, and E. Milella, "Surface and biological evaluation of hydroxyapatite-based coatings on titanium deposited by different techniques," *J. Biomed. Mater. Res.*, vol. 58, no. 6, pp. 651–657, 2001, doi: 10.1002/jbm.1065.

[75] T. Ogawa, L. Saruwatari, K. Takeuchi, H. Aita, and N. Ohno, "Ti nano-nodular structuring for bone integration and regeneration," *J. Dent. Res.*, vol. 87, no. 8, pp. 751–756, 2008, doi: 10.1177/154405910808700809.

[76] R. Brånemark, L. Emanuelsson, A. Palmquist, and P. Thomsen, "Bone response to laser-induced micro- and nano-size titanium surface features," *Nanomedicine Nanotechnology, Biol. Med.*, vol. 7, no. 2, pp. 220–227, 2011, doi: 10.1016/j.nano.2010.10.006.

[77] T. A. B. Bressel *et al.*, "Laser-modified titanium surfaces enhance the osteogenic differentiation of human mesenchymal stem cells," *Stem Cell Res. Ther.*, vol. 8, no. 1, pp. 1–11, Nov. 2017, doi: 10.1186/S13287-017-0717-9/FIGURES/8.

[78] Y. L. Jung and H. J. Donahue, “Cell sensing and response to micro- and nanostructured surfaces produced by chemical and topographic patterning,” *Tissue Eng.*, vol. 13, no. 8, pp. 1879–1891, 2007, doi: 10.1089/ten.2006.0154.

[79] 1 Antonio Nanci Paulo Tambasco de Oliveira, 1 Sylvia Francis Zalzal, 2 Marcio Mateus Beloti, 1 Adalberto Luiz Rosa, “Enhancement of in vitro osteogenesis on titanium by chemically produced nanotopography,” *J. Biomed. Mater. Res. Part A*, vol. 79, no. 4, pp. 963–73, 2006, doi: 10.1002/jbm.a.

[80] I. Demetrescu, D. Ionita, C. Pirvu, and D. Portan, “Present and Future Trends in TiO 2 Nanotubes Elaboration, Characterization and Potential Applications,” *Mol. Cryst. Liq. Cryst.*, vol. 521, no. 1, pp. 195–203, 2010, doi: 10.1080/15421401003715918.

[81] K. C. Popat, L. Leoni, C. A. Grimes, and T. A. Desai, “Influence of engineered titania nanotubular surfaces on bone cells,” *Biomaterials*, vol. 28, no. 21, pp. 3188–3197, Jul. 2007, doi: 10.1016/J.BIOMATERIALS.2007.03.020.

[82] R. Zahran, J. I. Rosales Leal, M. A. Rodríguez Valverde, and M. A. Cabrerizo Vílchez, “Effect of Hydrofluoric Acid Etching Time on Titanium Topography, Chemistry, Wettability, and Cell Adhesion,” 2016, doi: 10.1371/journal.pone.0165296.

[83] J. Lario, A. Amigó, F. I. Segovia, and V. I. Amigó, “materials Surface Modification of Ti-35Nb-10Ta-1.5Fe by the Double Acid-Etching Process,” 2018, doi: 10.3390/ma11040494.

[84] P. Tambasco De Oliveira and A. Nanci, “Nanotexturing of titanium-based surfaces upregulates expression of bone sialoprotein and osteopontin by cultured osteogenic cells,” *Biomaterials*, vol. 25, no. 3, pp. 403–413, 2004, doi: 10.1016/S0142-9612(03)00539-8.

[85] A. J. Steeves, A. Atwal, S. C. Schock Cd, and F. Variola, “Evaluation of the direct effects of poly(dopamine) on the in vitro response of human osteoblastic cells,” *J. Mater. Chem. B*, vol. 4, p. 3145, 2016, doi: 10.1039/c5tb02510a.

[86] A. Rodriguez-Contreras, D. Guadarrama Bello, S. Flynn, F. Variola, J. D. Wuest, and A. Nanci, “Chemical nanocavitation of surfaces to enhance the utility of stainless steel as a medical material,” *Colloids Surfaces B Biointerfaces*, vol. 161, pp. 677–687, Jan. 2018, doi: 10.1016/J.COLSURFB.2017.11.051.

[87] “getfile.” .

[88] F. Variola, S. Francis-Zalzal, A. Leduc, J. Barbeau, and A. Nanci, “Oxidative nanopatterning of titanium generates mesoporous surfaces with antimicrobial properties,” *Int. J. Nanomedicine*, p. 2319, May 2014, doi: 10.2147/IJN.S61333.

[89] M. B. Ariganello *et al.*, “Surface nanocavitation of titanium modulates macrophage activity,” *Int. J. Nanomedicine*, vol. 13, pp. 8297–8308, 2018, doi: 10.2147/IJN.S185436.

[90] C. Pautke *et al.*, “Characterization of osteosarcoma cell lines MG-63, Saos-2 and U-2 OS in comparison to human osteoblasts,” *Anticancer Res.*, vol. 24, no. 6, pp. 3743–3748, 2004.

[91] E. M. Czekanska, M. J. Stoddart, J. R. Ralphs, R. G. Richards, and J. S. Hayes, “A phenotypic comparison of osteoblast cell lines versus human primary osteoblasts for biomaterials testing,” *J. Biomed. Mater. Res. Part A*, vol. 102, no. 8, pp. 2636–2643, Aug. 2014, doi: 10.1002/JBM.A.34937.

[92] E. M. Czekanska, M. J. Stoddart, R. G. Richards, and J. S. Hayes, “In search of an osteoblast cell model for in vitro research,” *Eur. Cells Mater.*, vol. 24, pp. 1–17, 2012, doi: 10.22203/eCM.v024a01.

[93] N. Shams, M. Ghasemi, S. Sadatmansouri, S. Bonakdar, and M. Ghasemi, “Morphology and Differentiation of MG63 Osteoblast Cells on Saliva Contaminated Implant Surfaces,” *J. Dent. (Tehran).*, vol. 12, no. 6, p. 424, Jun. 2015, Accessed: Jan. 20, 2023. [Online]. Available: /pmc/articles/PMC4754568/.

[94] X. Shao, X. Cao, G. Song, Y. Zhao, and B. Shi, “Metformin Rescues the MG63 Osteoblasts against the Effect of High Glucose on Proliferation,” *J. Diabetes Res.*, vol. 2014, 2014, doi: 10.1155/2014/453940.

[95] M. Salerno *et al.*, “Pubertal Growth, Sexual Maturation, and Final Height in Children With IDDM: Effects of age at onset and metabolic control,” *Diabetes Care*, vol. 20, no. 5, pp. 721–724, May 1997, doi: 10.2337/DIACARE.20.5.721.

[96] D. Lozano *et al.*, “Role of parathyroid hormone-related protein in the decreased osteoblast function in diabetes-related osteopenia,” *Endocrinology*, vol. 150, no. 5, pp. 2027–2035, May 2009, doi: 10.1210/EN.2008-1108.

[97] R. E. Weiss, A. H. Gorn, and M. E. Nimni, “Abnormalities in the biosynthesis of cartilage and bone proteoglycans in experimental diabetes,” *Diabetes*, vol. 30, no. 8, pp. 670–677, 1981, doi: 10.2337/DIAB.30.8.670.

[98] N. P. Bueno *et al.*, “Photobiomodulation treatments drive osteogenic versus adipocytic fate of bone marrow mesenchymal stem cells reversing the effects of hyperglycemia in diabetes,” *Lasers Med. Sci.*, doi: 10.1007/s10103-022-03553-9.

[99] B. Valdez-Salas *et al.*, “Recovering Osteoblast Functionality on TiO2 Nanotube Surfaces Under Diabetic Conditions,” *Int. J. Nanomedicine*, vol. 17, no. November, pp.

5469–5488, 2022, doi: 10.2147/IJN.S387386.

[100] T. Komori, "Regulation of osteoblast differentiation by transcription factors," *J. Cell. Biochem.*, vol. 99, no. 5, pp. 1233–1239, 2006, doi: 10.1002/jcb.20958.

[101] T. M. Schroeder, E. D. Jensen, and J. J. Westendorf, "Runx2: A master organizer of gene transcription in developing and maturing osteoblasts," *Birth Defects Res. Part C - Embryo Today Rev.*, vol. 75, no. 3, pp. 213–225, 2005, doi: 10.1002/bdrc.20043.

[102] J. L. Fowlkes *et al.*, "Runt-Related Transcription Factor 2 (RUNX2) and RUNX2-Related Osteogenic Genes Are Down-Regulated throughout Osteogenesis in Type 1 Diabetes Mellitus," *Endocrinology*, vol. 149, no. 4, pp. 1697–1704, Apr. 2008, doi: 10.1210/EN.2007-1408.

[103] S. Pasricha, "Research Article Research Article," *Arch. Anesthesiol. Crit. Care*, vol. 4, no. 4, pp. 527–534, 2020.

[104] H. Lu, D. Kraut, L. C. Gerstenfeld, and D. T. Graves, "Diabetes interferes with the bone formation by affecting the expression of transcription factors that regulate osteoblast differentiation," *Endocrinology*, vol. 144, no. 1, pp. 346–352, 2003, doi: 10.1210/en.2002-220072.

[105] Z. Liu *et al.*, "Different concentrations of glucose regulate proliferation and osteogenic differentiation of osteoblasts Via the PI3 Kinase/Akt Pathway," *Implant Dent.*, vol. 24, no. 1, pp. 83–91, 2015, doi: 10.1097/ID.0000000000000196.

[106] S. Trivedi *et al.*, "A quantitative method to determine osteogenic differentiation aptness of scaffold," *J. Oral Biol. Craniofacial Res.*, vol. 10, no. 2, p. 158, Apr. 2020, doi: 10.1016/J.JOBCR.2020.04.006.

[107] S. Botolin and L. R. McCabe, "Chronic hyperglycemia modulates osteoblast gene expression through osmotic and non-osmotic pathways," *J. Cell. Biochem.*, vol. 99, no. 2, pp. 411–424, 2006, doi: 10.1002/jcb.20842.

[108] S. C. Moser and B. C. J. van der Eerden, "Osteocalcin — A versatile bone-derived hormone," *Front. Endocrinol. (Lausanne).*, vol. 10, no. JAN, pp. 4–9, 2019, doi: 10.3389/fendo.2018.00794.

[109] B. Knepper-Nicolai, A. Reinstorf, I. Hofinger, K. Flade, R. Wenz, and W. Pompe, "Influence of osteocalcin and collagen I on the mechanical and biological properties of Biocement D," *Biomol. Eng.*, vol. 19, no. 2–6, pp. 227–231, Aug. 2002, doi: 10.1016/S1389-0344(02)00036-9.

[110] J. Verhaeghe, E. Van Herck, R. Van Bree, K. Moermans, and R. Bouillon, "Decreased osteoblast activity in spontaneously diabetic rats: In vivo studies on the pathogenesis,"

Endocrine, vol. 7, no. 2, pp. 165–175, 1997, doi: 10.1007/BF02778138/METRICS.

[111] J. Wei and G. Karsenty, "An overview of the metabolic functions of osteocalcin," *Rev. Endocr. Metab. Disord.*, vol. 16, no. 2, pp. 93–98, Jul. 2015, doi: 10.1007/S11154-014-9307-7.

[112] J. Yang *et al.*, "Tio2 nanotubes alleviate diabetes-induced osteogenetic inhibition," *Int. J. Nanomedicine*, vol. 15, pp. 3523–3537, 2020, doi: 10.2147/IJN.S237008.

[113] K. Im, S. Mareninov, M. Fernando, P. Diaz, and W. H. Yong, "Chapter 26 An Introduction to Performing Immunofluorescence Staining," doi: 10.1007/978-1-4939-8935-5_26.

[114] D. C. Sun *et al.*, "In vitro culture and characterization of alveolar bone osteoblasts isolated from type 2 diabetics," *Brazilian J. Med. Biol. Res.*, vol. 45, no. 6, pp. 502–509, 2012, doi: 10.1590/S0100-879X2012007500054.

[115] T. Scholzen and J. Gerdes, "The Ki-67 protein: From the known and the unknown," *J. Cell. Physiol.*, vol. 182, no. 3, pp. 311–322, 2000, doi: 10.1002/(SICI)1097-4652(200003)182:3<311::AID-JCP1>3.0.CO;2-9.

[116] S. S. Menon, C. Guruvayoorappan, K. M. Sakthivel, and R. R. Rasmi, "Ki-67 protein as a tumour proliferation marker," *Clin. Chim. Acta*, vol. 491, no. November 2018, pp. 39–45, 2019, doi: 10.1016/j.cca.2019.01.011.

[117] P. Jalava, T. Kuopio, L. Juntti-Patinen, T. Kotkansalo, P. Kronqvist, and Y. Collan, "Ki67 immunohistochemistry: A valuable marker in prognostication but with a risk of misclassification: Proliferation subgroups formed based on Ki67 immunoreactivity and standardized mitotic index," *Histopathology*, vol. 48, no. 6, pp. 674–682, 2006, doi: 10.1111/j.1365-2559.2006.02402.x.

[118] E. Klæstad, S. Opdahl, S. X. Raj, A. M. Bofin, and M. Valla, "Long term trends of breast cancer incidence according to proliferation status," *BMC Cancer*, vol. 22, no. 1, pp. 1–12, 2022, doi: 10.1186/s12885-022-10438-1.

[119] S. N. Nayab, F. H. Jones, and I. Olsen, "Modulation of the human bone cell cycle by calcium ion-implantation of titanium," *Biomaterials*, vol. 28, no. 1, pp. 38–44, 2007, doi: 10.1016/j.biomaterials.2006.08.032.

[120] S. Vimalraj, B. Arumugam, P. J. Miranda, and N. Selvamurugan, "Runx2: Structure, function, and phosphorylation in osteoblast differentiation," *Int. J. Biol. Macromol.*, vol. 78, pp. 202–208, 2015, doi: 10.1016/j.ijbiomac.2015.04.008.

[121] A. L. Boskey, F. H. Wians, and P. V. Hauschka, "The effect of osteocalcin on in vitro lipid-induced hydroxyapatite formation and seeded hydroxyapatite growth," *Calcif.*

Tissue Int., vol. 37, no. 1, pp. 57–62, Jan. 1985, doi: 10.1007/BF02557680.

[122] L. Sun *et al.*, "Controlling growth and osteogenic differentiation of osteoblasts on microgrooved polystyrene surfaces," *PLoS One*, vol. 11, no. 8, pp. 1–15, 2016, doi: 10.1371/journal.pone.0161466.

[123] M. Sonnaert, I. Papantoniou, F. P. Luyten, and J. Schrooten, "Quantitative Validation of the Presto Blueä Metabolic Assay for Online Monitoring of Cell Proliferation in a 3D Perfusion Bioreactor System," doi: 10.1089/ten.tec.2014.0255.

[124] K. L. McKinley *et al.*, "Cellular aspect ratio and cell division mechanics underlie the patterning of cell progeny in diverse mammalian epithelia," *Elife*, vol. 7, Jun. 2018, doi: 10.7554/ELIFE.36739.

[125] A. Azizullah and D. P. Häder, "Ecotox," *Bioassays Adv. Methods Appl.*, pp. 199–219, Jan. 2018, doi: 10.1016/B978-0-12-811861-0.00010-3.

[126] "The difference in eccentricity for normal red blood cell and... | Download Scientific Diagram." https://www.researchgate.net/figure/The-difference-in-eccentricity-for-normal-red-blood-cell-and-sickle-shaped-red-blood_fig1_332381455 (accessed Jan. 28, 2023).

[127] I. C. Ng, P. Pawijit, J. Tan, and H. Yu, "Anatomy and Physiology for Biomaterials Research and Development," *Encycl. Biomed. Eng.*, vol. 1–3, pp. 225–236, Jan. 2019, doi: 10.1016/B978-0-12-801238-3.99876-3.

[128] L. Krishna *et al.*, "Nanostructured scaffold as a determinant of stem cell fate," *Stem Cell Res. Ther. 2016 71*, vol. 7, no. 1, pp. 1–12, Dec. 2016, doi: 10.1186/S13287-016-0440-Y.

[129] M. Rubert and C. de la Piedra, "Osteocalcin: From marker of bone formation to hormone; and bone, an endocrine organ," *Rev. Osteoporos. y Metab. Miner.*, vol. 12, no. 4, pp. 146–151, 2021, doi: 10.4321/S1889-836X2020000400007.

Chapter 7

APPENDIX

Appendix A:

ELSEVIER LICENSE
TERMS AND CONDITIONS

Apr 05, 2023

This Agreement between Ms. Nidhi Agrawal ("You") and Elsevier ("Elsevier") consists of your license details and the terms and conditions provided by Elsevier and Copyright Clearance Center.

License Number	5522781067609
License date	Apr 05, 2023
Licensed Content Publisher	Elsevier
Licensed Content Publication	Surface Science
Licensed Content Title	Characterization of a bioactive nanotextured surface created by controlled chemical oxidation of titanium
Licensed Content Author	Ji-Hyun Yi,Caroline Bernard,Fabio Variola,Sylvia F. Zalzal,James D. Wuest,Federico Rosei,Antonio Nanci
Licensed Content Date	Oct 1, 2006
Licensed Content Volume	600
Licensed Content Issue	19
Licensed Content Pages	9
Start Page	4613
End Page	4621
Type of Use	reuse in a thesis/dissertation

Appendix B:

JOHN WILEY AND SONS LICENSE
TERMS AND CONDITIONS

Apr 05, 2023

This Agreement between Ms. Nidhi Agrawal ("You") and John Wiley and Sons ("John Wiley and Sons") consists of your license details and the terms and conditions provided by John Wiley and Sons and Copyright Clearance Center.

License Number	5522800211713
License date	Apr 05, 2023
Licensed Content Publisher	John Wiley and Sons
Licensed Content Publication	Advanced Materials
Licensed Content Title	Surface Nanopatterning to Control Cell Growth
Licensed Content Author	Ludovic Richert, Fiorenzo Vetrone, Ji-Hyun Yi, et al
Licensed Content Date	Apr 21, 2008
Licensed Content Volume	20
Licensed Content Issue	8
Licensed Content Pages	5
Type of use	Dissertation/Thesis
Requestor type	University/Academic
Format	Electronic

Appendix C:

Nanoscale Oxidative Patterning of Metallic Surfaces to Modulate Cell Activity and Fate

Author: Fiorenzo Vetrone, Fabio Variola, Paulo Tambasco de Oliveira, et al

Publication: Nano Letters

Publisher: American Chemical Society

Date: Feb 1, 2009

PERMISSION/LICENSE IS GRANTED FOR YOUR ORDER AT NO CHARGE

This type of permission/license, instead of the standard Terms and Conditions, is sent to you because no fee is being charged for your order. Please note the following:

- Permission is granted for your request in both print and electronic formats, and translations.
- If figures and/or tables were requested, they may be adapted or used in part.
- Please print this page for your records and send a copy of it to your publisher/graduate school.
- Appropriate credit for the requested material should be given as follows: "Reprinted (adapted) with permission from {COMPLETE REFERENCE CITATION}. Copyright {YEAR} American Chemical Society." Insert appropriate information in place of the capitalized words.
- One-time permission is granted only for the use specified in your RightsLink request. No additional uses are granted (such as derivative works or other editions). For any uses, please submit a new request.

If credit is given to another source for the material you requested from RightsLink, permission must be obtained from that source.

Appendix D:

OXFORD UNIVERSITY PRESS LICENSE
TERMS AND CONDITIONS

Apr 05, 2023

This Agreement between Ms. Nidhi Agrawal ("You") and Oxford University Press ("Oxford University Press") consists of your license details and the terms and conditions provided by Oxford University Press and Copyright Clearance Center.

License Number	5522841342694
License date	Apr 05, 2023
Licensed content publisher	Oxford University Press
Licensed content publication	Endocrinology
Licensed content title	Diabetes Interferes with the Bone Formation by Affecting the Expression of Transcription Factors that Regulate Osteoblast Differentiation
Licensed content author	Lu, Huafei; Kraut, Douglas
Licensed content date	Jan 1, 2003
Type of Use	Thesis/Dissertation
Institution name	
Title of your work	Understanding the effects of nanoporous titanium on osteoblastic cells in hyperglycemic conditions
Publisher of your work	University of Ottawa

Appendix E:

JOHN WILEY AND SONS LICENSE
TERMS AND CONDITIONS

Apr 05, 2023

This Agreement between Ms. Nidhi Agrawal ("You") and John Wiley and Sons ("John Wiley and Sons") consists of your license details and the terms and conditions provided by John Wiley and Sons and Copyright Clearance Center.

License Number	5522850129941
License date	Apr 05, 2023
Licensed Content Publisher	John Wiley and Sons
Licensed Content Publication	Journal of Cellular Biochemistry
Licensed Content Title	Chronic hyperglycemia modulates osteoblast gene expression through osmotic and non-osmotic pathways
Licensed Content Author	Laura R. McCabe, Sergiu Botolin
Licensed Content Date	Apr 17, 2006
Licensed Content Volume	99
Licensed Content Issue	2
Licensed Content Pages	14
Type of use	Dissertation/Thesis
Requestor type	University/Academic
Format	Electronic